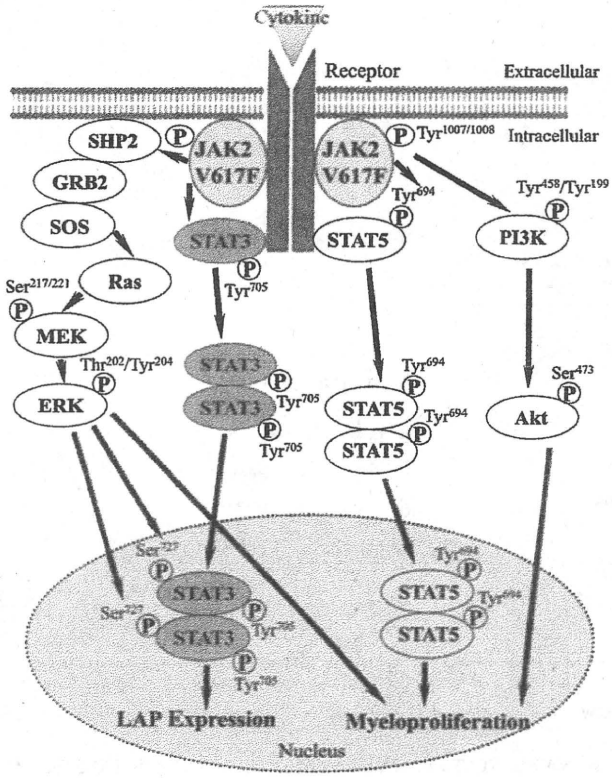

Fig 7. Schematic presentation of JAK2 V617F signalling to activate myeloproliferation and LAP expression. The activated JAK2 kinase induces STAT3/STAT5 tyrosine phosphorylation, and then phosphorylated STATs are dimerized, enter the nucleus, and bind specific regulatory sequences to regulate transcription of target genes. This pathway is a major downstream signalling cascade of JAK/STAT. Tyrosine phosphorylation of STAT5 mediates enhancing myeloproliferation. On the other hand, JAK2 also phosphorylates signalling molecules in Ras/MEK/ERK and PI3K/Akt pathways that are also responsible for cell proliferation. STAT3 has two phosphorylation sites, Tyr^{705} and Ser^{727}. Tyrosine phosphorylation is transduced by JAK2, whereas serine phosphorylation is transduced by MEK/ERK pathway. Serine phosphorylation of STAT3 probably affects the STAT3 transcriptional activation. JAK2 V617F stimulates the LAP expression also via MEK/ERK-dependent signalling pathway that phosphorylates STAT3 Ser^{727}. Thus, JAK2 V617F uses STAT3 pathway to induce LAP expression, and STAT5, Ras/MEK/ERK and PI3K/Akt pathways to stimulate myeloproliferation.

showed that both pathways are responsible for cell proliferation. STAT3 siRNA and the MEK1/2 inhibitor U0126 significantly reduced LAP expression (Figs 4A, 5A, E). Furthermore, U0126 not only inhibited ERK phosphorylation but also STAT3 Ser^{727} phosphorylation (Fig 5B). STAT3 has two phosphorylation sites, which are Tyr^{705} and Ser^{727} sites. Tyrosine phosphorylation of STAT3 is the major signalling cascade of JAK/STAT pathway described above. On the other hand, serine phosphorylation of STAT3 probably affects the STAT3 transcriptional activation, which is mainly transduced by the MEK/ERK pathway. In fact, a STAT3 S727A mutant, where Ser^{727} was replaced with an alanine, exhibited marked reduction in transcriptional activation, indicating that STAT3 Ser^{727} phosphorylation is essential for STAT3 transcriptional activation (Wen *et al*, 1995; Zhang *et al*, 1995). Consistent with this, LAP expression was suppressed significantly by STAT3 siRNA despite ERK phosphorylation (Fig 4A, B). The MEK/ERK signalling unrelated to STAT3 serine phosphorylation was not required for LAP expression. These findings show that STAT3 serine phosphorylation is mainly involved in enhancing LAP expression in Jak2 V617F signalling pathways.

JAK2 V617F mutation occurs at the HSC level (Jamieson *et al*, 2006; Kota *et al*, 2008). It is still unclear how this common mutation can induce three distinct MPN. Our data shows that the JAK2 V617F uses at least two distinct signalling pathways for enhancing LAP expression in neutrophil and cell proliferation of the myeloid lineage cell line (Fig 7). We and others have reported that the balance between constitutively activated STAT3/STAT5 or the expression level of JAK2 V617F could be a determinant for the type of MPN (Mesa *et al*, 2006; Teofili *et al*, 2007; Shide *et al*, 2008; Tiedt *et al*, 2008; Xing *et al*, 2008). To understand the developmental mechanisms of MPN, it is critical to understand the contribution of each signalling pathway toward the proliferation and lineage fate decision of HSCs in different types of MPN.

In conclusion, we obtained direct evidence that JAK2 V617F mainly induces elevation of LAP scores via the STAT3 pathway, whereas it stimulates cell proliferation via the STAT5, Ras/MEK/ERK and PI3K pathways. Thus, JAK2 V617F uses distinct signalling pathways to enhance LAP expression and myeloproliferation, typical characteristics in *BCR-ABL1* negative MPN.

Acknowledgements

This work was supported in part by a Grant-in-Aid from the Ministry of Education, Culture, Sports, Science and Technology in Japan (20591134[K.T.], 21659239[K.A.]), the Takeda Science Foundation [K.T.], and the Mitsubishi Pharma Research Foundation [K.T.].

References

Basquiera, A.L., Fassetta, F., Soria, N., Barral, J.M., Ricchi, B. & Garcia, J.J. (2007) Accuracy of leukocyte alkaline phosphatase score to predict JAK2 V617F mutation. *Haematologica*, **92**, 704–705.

Baxter, E.J., Scott, L.M., Campbell, P.J., East, C., Fourouclas, N., Swanton, S., Vassiliou, G.S., Bench, A.J., Boyd, E.M., Curtin, N., Scott, M.A., Erber, W.N. & Green, A.R. (2005) Acquired mutation of the tyrosine kinase JAK2 in human myeloproliferative disorders. *Lancet*, **365**, 1054–1061.

Borregaard, N. & Cowland, J.B. (1997) Granules of the human neutrophilic polymorphonuclear leukocyte. *Blood*, **89**, 3503–3521.

Borregaard, N., Miller, L.J. & Springer, T.A. (1987) Chemoattractant-regulated mobilization of a novel intracellular compartment in human neutrophils. *Science*, **237**, 1204–1206.

Borregaard, N., Kjeldsen, L., Rygaard, K., Bastholm, L., Nielsen, M.H., Sengelov, H., Bjerrum, O.W. & Johnsen, A.H. (1992) Stimulus-

dependent secretion of plasma proteins from human neutrophils. *Journal of Clinical Investigation*, **90**, 86–96.

Chung, J., Uchida, E., Grammer, T.C. & Blenis, J. (1997) STAT3 serine phosphorylation by ERK-dependent and -independent pathways negatively modulates its tyrosine phosphorylation. *Molecular and Cellular Biology*, **17**, 6508–6516.

Dameshek, W. (1951) Some speculations on the myeloproliferative syndromes. *Blood*, **6**, 372–375.

Dotti, G., Garattini, E., Borleri, G., Masuhara, K., Spinelli, O., Barbui, T. & Rambaldi, A. (1999) Leucocyte alkaline phosphatase identifies terminally differentiated normal neutrophils and its lack in chronic myelogenous leukaemia is not dependent on p210 tyrosine kinase activity. *British Journal of Haematology*, **105**, 163–172.

Falanga, A., Marchetti, M., Evangelista, V., Vignoli, A., Licini, M., Balicco, M., Manarini, S., Finazzi, G., Cerletti, C. & Barbui, T. (2000) Polymorphonuclear leukocyte activation and hemostasis in patients with essential thrombocythemia and polycythemia vera. *Blood*, **96**, 4261–4266.

Faurschou, M. & Borregaard, N. (2003) Neutrophil granules and secretory vesicles in inflammation. *Microbes and Infection*, **5**, 1317–1327.

Garattini, E. & Gianni, M. (1996) Leukocyte alkaline phosphatase a specific marker for the post-mitotic neutrophilic granulocyte: regulation in acute promyelocytic leukemia. *Leukaemia & Lymphoma*, **23**, 493–503.

Gianni, M., Terao, M., Zanotta, S., Barbui, T., Rambaldi, A. & Garattini, E. (1994) Retinoic acid and granulocyte colony-stimulating factor synergistically induce leukocyte alkaline phosphatase in acute promyelocytic leukemia cells. *Blood*, **83**, 1909–1921.

Hayhoe, F.G. & Quaglino, D. (1958) Cytochemical demonstration and measurement of leucocyte alkaline phosphatase activity in normal and pathological states by a modified azo-dye coupling technique. *British Journal of Haematology*, **4**, 375–389.

Ihle, J.N. (1995) Cytokine receptor signalling. *Nature*, **377**, 591–594.

Jain, N., Zhang, T., Fong, S.L., Lim, C.P. & Cao, X. (1998) Repression of Stat3 activity by activation of mitogen-activated protein kinase (MAPK). *Oncogene*, **17**, 3157–3167.

James, C., Ugo, V., Le Couedic, J.P., Staerk, J., Delhommeau, F., Lacout, C., Garcon, L., Raslova, H., Berger, R., Bennaceur-Griscelli, A., Villeval, J.L., Constantinescu, S.N., Casadevall, N. & Vainchenker, W. (2005) A unique clonal JAK2 mutation leading to constitutive signalling causes polycythaemia vera. *Nature*, **434**, 1144–1148.

Jamieson, C.H., Gotlib, J., Durocher, J.A., Chao, M.P., Mariappan, M.R., Lay, M., Jones, C., Zehnder, J.L., Lilleberg, S.L. & Weissman, I.L. (2006) The JAK2 V617F mutation occurs in hematopoietic stem cells in polycythemia vera and predisposes toward erythroid differentiation. *Proceedings of the National Academy of Sciences of the United States of America*, **103**, 6224–6229.

Jones, A.V., Kreil, S., Zoi, K., Waghorn, K., Curtis, C., Zhang, L., Score, J., Seear, R., Chase, A.J., Grand, F.H., White, H., Zoi, C., Loukopoulos, D., Terpos, E., Vervessou, E.C., Schultheis, B., Emig, M., Ernst, T., Lengfelder, E., Hehlmann, R., Hochhaus, A., Oscier, D., Silver, R.T., Reiter, A. & Cross, N.C. (2005) Widespread occurrence of the JAK2 V617F mutation in chronic myeloproliferative disorders. *Blood*, **106**, 2162–2168.

Kaplow, L.S. (1955) A histochemical procedure for localizing and evaluating leukocyte alkaline phosphatase activity in smears of blood and marrow. *Blood*, **10**, 1023–1029.

Kaplow, L.S. (1963) Cytochemistry of leukocyte alkaline phosphatase. Use of complex naphthol as phosphates in azo dyecoupling technics. *American Journal of Clinical Pathology*, **39**, 439–449.

Kondo, T., Okuno, N., Naruse, H., Kishimoto, M., Tasaka, T., Tsujioka, T., Matsuoka, A., Sugihara, T., Tohyama, Y. & Tohyama, K. (2008) Validation of the revised 2008 WHO diagnostic criteria in 75 suspected cases of myeloproliferative neoplasm. *Leukaemia & Lymphoma*, **49**, 1784–1791.

Kota, J., Caceres, N. & Constantinescu, S.N. (2008) Aberrant signal transduction pathways in myeloproliferative neoplasms. *Leukemia*, **22**, 1828–1840.

Kralovics, R., Passamonti, F., Buser, A.S., Teo, S.S., Tiedt, R., Passweg, J.R., Tichelli, A., Cazzola, M. & Skoda, R.C. (2005) A gain-of-function mutation of JAK2 in myeloproliferative disorders. *New England Journal of Medicine*, **352**, 1779–1790.

Lacout, C., Pisani, D.F., Tulliez, M., Gachelin, F.M., Vainchenker, W. & Villeval, J.L. (2006) JAK2V617F expression in murine hematopoietic cells leads to MPD mimicking human PV with secondary myelofibrosis. *Blood*, **108**, 1652–1660.

Levine, R.L. & Wernig, G. (2006) Role of JAK-STAT signaling in the pathogenesis of myeloproliferative disorders. *Hematology/the Education Program of the American Society of Hematology. American Society of Hematology. Education Program*, **2006**, 233–239.

Levine, R.L., Wadleigh, M., Cools, J., Ebert, B.L., Wernig, G., Huntly, B.J., Boggon, T.J., Wlodarska, I., Clark, J.J., Moore, S., Adelsperger, J., Koo, S., Lee, J.C., Gabriel, S., Mercher, T., D'Andrea, A., Frohling, S., Dohner, K., Marynen, P., Vandenberghe, P., Mesa, R.A., Tefferi, A., Griffin, J.D., Eck, M.J., Sellers, W.R., Meyerson, M., Golub, T.R., Lee, S.J. & Gilliland, D.G. (2005) Activating mutation in the tyrosine kinase JAK2 in polycythemia vera, essential thrombocythemia, and myeloid metaplasia with myelofibrosis. *Cancer Cell*, **7**, 387–397.

Mesa, R.A., Tefferi, A., Lasho, T.S., Loegering, D., McClure, R.F., Powell, H.L., Dai, N.T., Steensma, D.P. & Kaufmann, S.H. (2006) Janus kinase 2 (V617F) mutation status, signal transducer and activator of transcription-3 phosphorylation and impaired neutrophil apoptosis in myelofibrosis with myeloid metaplasia. *Leukemia*, **20**, 1800–1808.

Parganas, E., Wang, D., Stravopodis, D., Topham, D.J., Marine, J.C., Teglund, S., Vanin, E.F., Bodner, S., Colamonici, O.R., van Deursen, J.M., Grosveld, G. & Ihle, J.N. (1998) Jak2 is essential for signaling through a variety of cytokine receptors. *Cell*, **93**, 385–395.

Passamonti, F., Rumi, E., Pietra, D., Della Porta, M.G., Boveri, E., Pascutto, C., Vanelli, L., Arcaini, L., Burcheri, S., Malcovati, L., Lazzarino, M. & Cazzola, M. (2006) Relation between JAK2 (V617F) mutation status, granulocyte activation, and constitutive mobilization of CD34+ cells into peripheral blood in myeloproliferative disorders. *Blood*, **107**, 3676–3682.

Sakamoto, S. (1966) Histochemical studies on leukocyte alkaline phosphatase activity with special reference to various types of hemolytic disorders. *Tohoku Journal of Experimental Medicine*, **89**, 387–399.

Sato, N., Takahashi, Y. & Asano, S. (1994) Preferential usage of the bone-type leader sequence for the transcripts of liver/bone/kidney-type alkaline phosphatase gene in neutrophilic granulocytes. *Blood*, **83**, 1093–1101.

Sengupta, T.K., Talbot, E.S., Scherle, P.A. & Ivashkiv, L.B. (1998) Rapid inhibition of interleukin-6 signaling and Stat3 activation mediated by mitogen-activated protein kinases. *Proceedings of the*

National Academy of Sciences of the United States of America, **95**, 11107–11112.

Shibano, M., Machii, T., Nishimori, Y., Nakamoto, I., Ueda, E., Masuhara, K. & Kitani, T. (1999) Assessment of alkaline phosphatase on the surface membrane of neutrophils by immunofluorescence. *American Journal of Hematology*, **60**, 12–18.

Shibata, A., Bennett, J.M., Castoldi, G.L., Catovsky, D., Flandrin, G., Jaffe, E.S., Katayama, I., Nanba, K., Schmalzl, F. & Yam, L.T. (1985) Recommended methods for cytological procedures in haematology. International Committee for Standardization in Haematology (ICSH). *Clinical and Laboratory Haematology*, **7**, 55–74.

Shide, K., Shimoda, K., Kamezaki, K., Kakumitsu, H., Kumano, T., Numata, A., Ishikawa, F., Takenaka, K., Yamamoto, K., Matsuda, T. & Harada, M. (2007) Tyk2 mutation homologous to V617F Jak2 is not found in essential thrombocythaemia, although it induces constitutive signaling and growth factor independence. *Leukemia Research*, **31**, 1077–1084.

Shide, K., Shimoda, H.K., Kumano, T., Karube, K., Kameda, T., Takenaka, K., Oku, S., Abe, H., Katayose, K.S., Kubuki, Y., Kusumoto, K., Hasuike, S., Tahara, Y., Nagata, K., Matsuda, T., Ohshima, K., Harada, M. & Shimoda, K. (2008) Development of ET, primary myelofibrosis and PV in mice expressing JAK2 V617F. *Leukemia*, **22**, 87–95.

Stewart, C.A. (1974) Leucocyte alkaline phosphatase in myeloid maturation. *Pathology*, **6**, 287–293.

Sullivan, G.W., Donowitz, G.R., Sullivan, J.A. & Mandell, G.L. (1984) Interrelationships of polymorphonuclear neutrophil membrane-bound calcium, membrane potential, and chemiluminescence: studies in single living cells. *Blood*, **64**, 1184–1192.

Takenaka, K., Prasolava, T.K., Wang, J.C., Mortin-Toth, S.M., Khalouei, S., Gan, O.I., Dick, J.E. & Danska, J.S. (2007) Polymorphism in Sirpa modulates engraftment of human hematopoietic stem cells. *Nature Immunology*, **8**, 1313–1323.

Teofili, L., Martini, M., Cenci, T., Petrucci, G., Torti, L., Storti, S., Guidi, F., Leone, G. & Larocca, L.M. (2007) Different STAT-3 and STAT-5 phosphorylation discriminates among Ph-negative chronic myeloproliferative diseases and is independent of the V617F JAK-2 mutation. *Blood*, **110**, 354–359.

Tiedt, R., Hao-Shen, H., Sobas, M.A., Looser, R., Dirnhofer, S., Schwaller, J. & Skoda, R.C. (2008) Ratio of mutant JAK2-V617F to wild-type Jak2 determines the MPD phenotypes in transgenic mice. *Blood*, **111**, 3931–3940.

Weiss, M.J., Ray, K., Henthorn, P.S., Lamb, B., Kadesch, T. & Harris, H. (1988) Structure of the human liver/bone/kidney alkaline phosphatase gene. *Journal of Biological Chemistry*, **263**, 12002–12010.

Wen, Z., Zhong, Z. & Darnell, Jr, J.E. (1995) Maximal activation of transcription by Stat1 and Stat3 requires both tyrosine and serine phosphorylation. *Cell*, **82**, 241–250.

Wernig, G., Mercher, T., Okabe, R., Levine, R.L., Lee, B.H. & Gilliland, D.G. (2006) Expression of Jak2V617F causes a polycythemia vera-like disease with associated myelofibrosis in a murine bone marrow transplant model. *Blood*, **107**, 4274–4281.

Witthuhn, B.A., Quelle, F.W., Silvennoinen, O., Yi, T., Tang, B., Miura, O. & Ihle, J.N. (1993) JAK2 associates with the erythropoietin receptor and is tyrosine phosphorylated and activated following stimulation with erythropoietin. *Cell*, **74**, 227–236.

Xing, S., Wanting, T.H., Zhao, W., Ma, J., Wang, S., Xu, X., Li, Q., Fu, X., Xu, M. & Zhao, Z.J. (2008) Transgenic expression of JAK2V617F causes myeloproliferative disorders in mice. *Blood*, **111**, 5109–5117.

Zaleskas, V.M., Krause, D.S., Lazarides, K., Patel, N., Hu, Y., Li, S. & Van Etten, R.A. (2006) Molecular pathogenesis and therapy of polycythemia induced in mice by JAK2 V617F. *PLoS ONE*, **1**, e18.

Zhang, X., Blenis, J., Li, H.C., Schindler, C. & Chen-Kiang, S. (1995) Requirement of serine phosphorylation for formation of STAT-promoter complexes. *Science*, **267**, 1990–1994.

Zhong, Z., Wen, Z. & Darnell, Jr, J.E. (1994) Stat3: a STAT family member activated by tyrosine phosphorylation in response to epidermal growth factor and interleukin-6. *Science*, **264**, 95–98.

 DOI 10.1002/eji.201040688 Eur. J. Immunol. 2010. 40: 3570–3580

European Journal of Immunology

Functional involvement of Daxx in gp130-mediated cell growth and survival in BaF3 cells

Ryuta Muromoto[1], Makoto Kuroda[1], Sumihito Togi[1], Yuichi Sekine[1], Asuka Nanbo[1], Kazuya Shimoda[2], Kenji Oritani[3] and Tadashi Matsuda[1]

[1] Department of Immunology, Graduate School of Pharmaceutical Sciences, Hokkaido University, Kita-12 Nishi-6, Kita-Ku, Sapporo, Japan
[2] Department of Internal Medicine II, Faculty of Medicine, University of Miyazaki, Kihara, Kiyotake, Miyazaki, Japan
[3] Department of Hematology and Oncology, Graduate School of Medicine, Osaka University, 2-2 Yamada-oka, Suita, Osaka, Japan

Death domain-associated protein (Daxx) is a multifunctional protein that modulates both cell death and transcription. Several recent studies have indicated that Daxx is a mediator of lymphocyte death and/or growth suppression, although the detailed mechanism is unclear. Previously, we reported that Daxx suppresses IL-6 family cytokine-induced gene expression by interacting with STAT3. STAT3 is important for the growth and survival of lymphocytes; therefore, we here examined the role of Daxx in the gp130/STAT3-dependent cell growth/survival signals. We found that Daxx suppresses the gp130/STAT3-dependent cell growth and that Daxx endogenously interacts with STAT3 and inhibits the DNA-binding activity of STAT3. Moreover, small-interfering RNA-mediated knockdown of Daxx enhanced the expression of STAT3-target genes and accelerated the STAT3-mediated cell cycle progression. In addition, knockdown of Daxx-attenuated lactate dehydrogenase leakage from cells, indicating that Daxx positively regulates cell death during gp130/STAT3-mediated cell proliferation. Notably, Daxx specifically suppressed the levels of Bcl2 mRNA and protein, even in cytokine-unstimulated cells, indicating that Daxx regulates Bcl2 expression independently of activated STAT3. These results suggest that Daxx suppresses gp130-mediated cell growth and survival by two independent mechanisms: inhibition of STAT3-induced transcription and down-regulation of Bcl2 expression.

Key words: Cell death · Daxx · gp130 · IL-6 · STAT3

Introduction

Death domain-associated protein (Daxx) is a multifunctional protein that modulates both cell death and transcription [1]. Daxx is present in most cell types and is mainly located in the nucleus. Because previous studies have demonstrated that Daxx can bear both pro- and anti-cell-death activities depending on the stimulus and the cell type [1, 2], the precise role of Daxx, in particular its ability to promote or hinder cell death, remains controversial. Nevertheless, in lymphocytes, the following observations indicate that Daxx has pro-cell death and/or growth-suppressing functions. First, Daxx is induced by type I interferon in pro-B cells and is required for interferon-induced apoptosis [3]. Second, in Con A-stimulated splenocytes, Daxx up-regulation and interaction with PML correlate with the induction of B-cell apoptosis [4]. Third, CD40-induced proliferation is profoundly reduced in transgenic B cells over-expressing Daxx [5]. Fourth, analysis of T-cell-specific transgenic mice expressing a dominant negative form of Daxx (Daxx-DN)

Correspondence: Dr. Tadashi Matsuda
e-mail: tmatsuda@pharm.hokudai.ac.jp

has reveled that Daxx-DN protects activated T cells from Fas-induced cell death and that T-lymphocytes expressing Daxx-DN exhibit increased proliferative T-cell responses [6]. These findings have indicated that Daxx is a mediator of lymphocyte death and/or growth suppression. However, the precise mechanism of how Daxx affects cell survival remained unclear.

Daxx interacts with and regulates the transcriptional activities of several DNA-binding transcription factors, including ETS1 [7], PAX5 [8], Glucocorticoid receptor [9], RelA [10], RelB [11], TCF4 [12], SMAD4 [13], C/EBP [14], AIRE [15] and STAT3 [16]. Considering that Daxx binds histone deacetylases [17], DNA methyltransferases and their associated proteins [18–20], and the chromatin-modifying protein α-thalassemia syndrome protein [21, 22], it seems possible that Daxx regulates cellular processes by regulating transcription of specific genes under different conditions. We have previously shown that Daxx suppresses STAT3-mediated transcriptional activity and has a role in regulating IL-6 family cytokine signaling and gene induction in several cancer cell lines [16].

The IL-6 family of cytokines utilizes the membrane glycoprotein gp130 as a critical signal-transducing receptor component [23]. Dimerization of gp130 activates the JAK family of protein tyrosine kinases, which phosphorylate and activate cytoplasmic STAT3 [24, 25]. Activated STAT3 dimerizes and translocates to the nucleus where it binds to specific DNA response elements and induces expression of STAT3-regulated genes. STAT3 has been known to play critical roles in the regulation of various cellular events, malignancies and autoimmune diseases [26–28]. In lymphocyte proliferation, STAT3 activation is responsible for IL-6-dependent T-cell proliferation by preventing apoptosis [29] and STAT3 is also indispensable for IL-27-mediated cell proliferation [30]. Moreover, Chou *et al.* demonstrated that STAT3 is required for maintaining pro-B-cell survival and for efficient B lymphopoiesis [31].

In the present study, we examined the role of Daxx in the gp130/STAT3-mediated cell proliferation signal. We found that Daxx represses STAT3 activity through the inhibition of DNA-binding, thereby inhibiting cytokine-dependent growth and survival of BaF3 cells. Moreover, Daxx also regulates *Bcl2* gene expression independently of STAT3 regulation. These results suggest that Daxx exerts growth suppression through the modulation of transcription.

Results

Daxx suppresses gp130/STAT3-dependent cell proliferation

We used an IL-3-dependent mouse pro-B-cell line, BaF3-derived BaF-G133, as a model for gp130/STAT3-mediated cell proliferation. It has been reported that, in the absence of IL-3, G-CSF-treatment of BaF-G133 cells induces dimerization of GCSFR/gp130 chimeric receptors causing activation of STAT3 and STAT3-dependent cell growth [32].

To examine the role of Daxx in gp130/STAT3-mediated cell growth, we introduced siRNA against Daxx (siDaxx) into BaF-G133 cells. Daxx protein levels were significantly reduced by siDaxx, whereas siDaxx had no effect on the levels of STAT3 or β-actin (Fig. 1A). We then investigated whether this reduction of Daxx in BaF-G133 cells could affect the rate of cell proliferation. After transfection of siRNA, cells were washed in IL-3-free medium and incubated for 48 h in the absence or presence of G-CSF at various concentrations. Silencing of endogenous Daxx by siRNA significantly enhanced the proliferation of BaF-G133 cells at all G-CSF concentrations tested (Fig. 1B). To further elucidate the role of Daxx in gp130/STAT3-mediated cell growth, we established BaF-G133 transfectants over-expressing Daxx

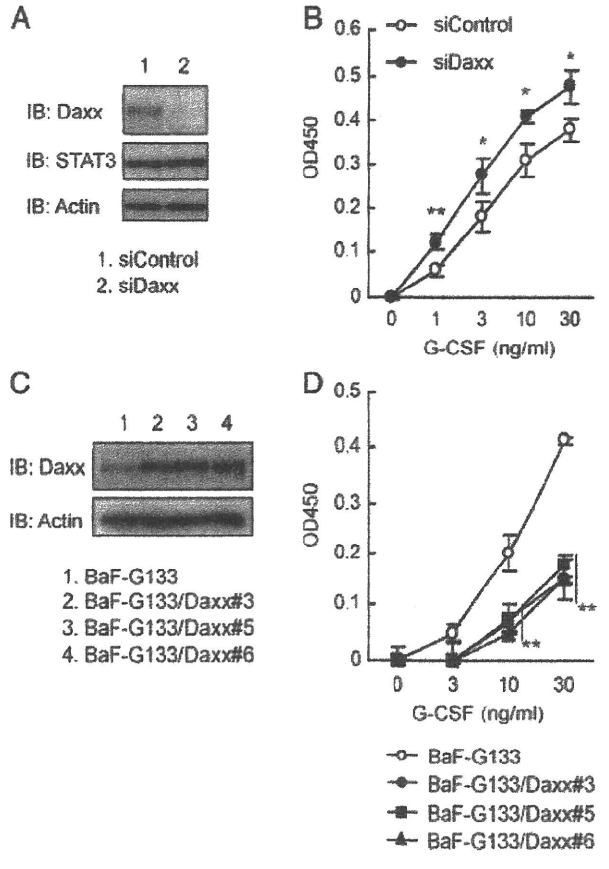

Figure 1. Involvement of Daxx protein in the regulation of gp130/STAT3-dependent cell proliferation. (A) BaF-G133 cells were transfected with Daxx-specific and control siRNA and Daxx knockdown was validated by western blot analysis of Daxx, STAT3 and β-actin. Knockdown of Daxx was comfirmed until 3 days after siRNA transfection. Data are representative of three independent experiments. (B) G-CSF-induced cell proliferation of control or Daxx siRNA transfected BaF-G133 cells was determined by the WST8 assay. Data show mean±SD of triplicate samples and representative of three independent experiments. $^{*}p<0.05$ and $^{**}p<0.01$ (Student's t-test). (C) Lysates from stable transfectants of BaF-G133 cells over-expressing Daxx were subjected to western blot analysis of Daxx and β-actin. Data are representative of three independent experiments. (D) The WST8 assay was performed on BaF-G133 cells and Daxx transfectants. Data show mean±SD of triplicate samples and representative of three independent experiments. $^{**}p<0.01$ (Student's t-test).

(Fig. 1C; BaF-G133/Daxx#3, BaF-G133/Daxx#5, BaF-G133/Daxx#6) and performed growth assays in the presence or absence of either G-CSF. Over-expression of Daxx caused a reduction in cell number when cells were stimulated with G-CSF (Fig. 1D). These results indicated that Daxx has the ability to suppress the gp130/STAT3-mediated cell growth.

Daxx suppresses cell cycle progression in BaF-G133 cells

To clarify how Daxx regulates cell proliferation, we examined whether gp130-induced cell cycle progression could be affected by knockdown of Daxx. After transfection of siControl or siDaxx, BaF-G133 cells were synchronized in G0/G1 by withdrawing IL-3 and cells were then treated with G-CSF. Cells were fixed and stained with propidium iodide and then DNA content *per* cell was determined by flow cytometry. As shown in Fig. 2A, BaF-G133 cells transfected with Daxx siRNA exhibited a significant acceleration in gp130-induced cell cycle progression to S and G2/M phases compared with those transfected with control siRNA.

Daxx increases cell death in BaF-G133 cells

Daxx has been reported to positively or negatively regulate cell death [1, 2]. Thus, we tested whether Daxx is involved in the regulation of cell death in BaF-G133 cells. Leakage of lactate dehydrogenase (LDH) into the medium was used as a marker for membrane breakage and cell death. In cells transfected with control siRNA and cultured without IL-3,

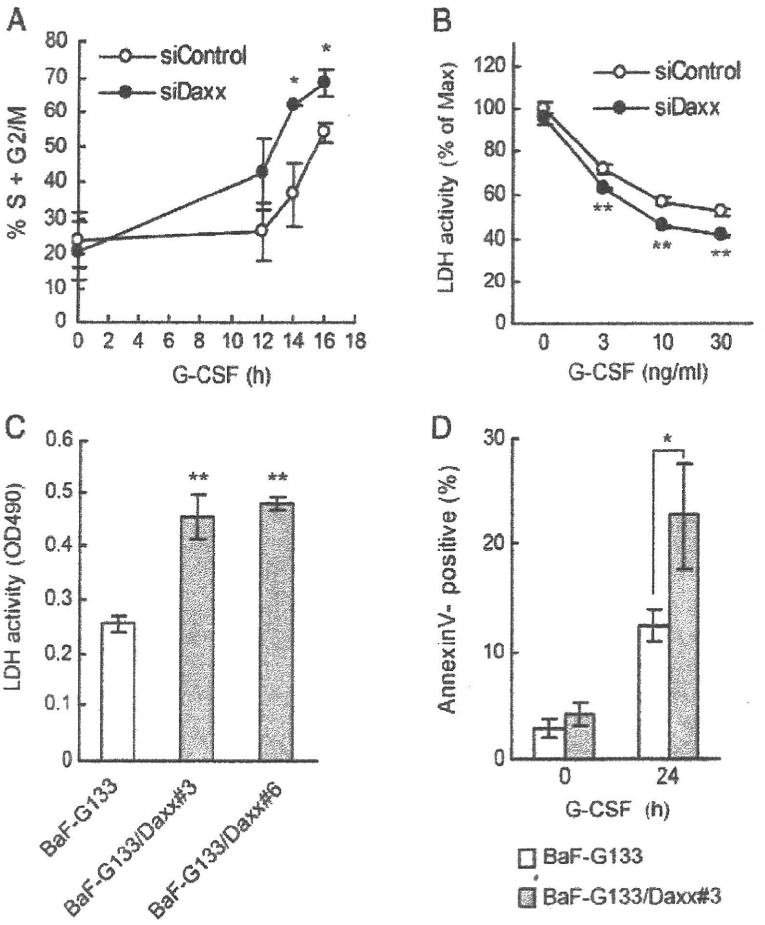

Figure 2. Daxx regulates cell cycle progression and cell death during gp130/STAT3-dependent cell growth. (A) BaF-G133 cells were treated with control siRNA or Daxx siRNA. Cells were IL-3-starved for 12 h and then treated with 30 ng/ml. G-CSF for the indicated times. Cells were then fixed and subjected to cell cycle analysis using FACS. The percentages of cells in S plus G2/M phases of the cell cycle are indicated (mean ± SD, $n = 3$). *$p<0.05$ (Student's t-test). (B) Daxx knockdown and control cells were cultured with the indicated concentrations of G-CSF for 48 h and the effect of Daxx knockdown on the G-CSF-induced reduction in cell death of BaF-G133 cells was evaluated by LDH activity in cell culture supernatants. Results are presented as the percentage of the maximum LDH release observed in untreated control cells (mean ± SD, $n = 3$). **$p<0.01$ (Student's t-test). (C) The LDH assay was performed on BaF-G133 cells and Daxx transfectants, cultured with 30 ng/mL of G-CSF for 48 h. Results are presented as OD at 490 nm (Mean ± SD, $n = 3$). **$p<0.01$ (Student's t-test). (D) BaF-G133 and BaF-G133/Daxx#3 cells were treated with 30 ng/mL G-CSF for the indicated times and the percentages of Annexin-V-positive cells were determined by FACS analysis (Mean ± SD, $n = 3$). *$p<0.05$ (Student's t-test).

G-CSF treatment, in a concentration-dependent manner, increased the number of viable cells (as shown in Fig. 1B) with a concomitant reduction of cell death, (Fig. 2B, open circle). Knockdown of endogenous Daxx significantly augmented G-CSF-induced reduction of LDH leakage compared with control cells (Fig. 2B, closed circle).

LDH leakage was increased by about 1.8-fold in Daxx over-expressing transfectants compared with control BaF-G133 cells (Fig. 2C). In addition, BaF-G133/Daxx#3 cells exhibited an increased percentage of Annexin-V-positive cells compared with control BaF-G133 cells (Fig. 2D).

These results indicated that Daxx has the ability to suppress cell cycle progression and to increase cell death, thereby controlling cell proliferation in BaF-G133 cells.

Daxx binds to STAT3 and inhibits its activity

We previously showed that Daxx interacts with STAT3 in transiently transfected 293T cells [16]. STAT3 is essential for gp130-mediated G1 to S phase transition in BaF-G133 cells [33]; therefore, we considered STAT3 to be a potential target of the anti-proliferative function of Daxx. To test whether a Daxx-STAT3 interaction occurs in BaF-G133 cells, we performed co-immunoprecipitation assays (Fig. 3A). An anti-Daxx antibody, but not control rabbit IgG, co-immunoprecipitated endogenous STAT3, regardless of G-CSF stimulation. These data suggest that Daxx endogenously forms a complex with STAT3 in BaF-G133 cells in a constitutive manner.

We next tested whether Daxx affects gp130-mediated phosphorylation of STAT3 and ERK/MAPK. We found that the gp130-mediated upregulation of STAT3 or ERK/MAPK phosphorylation in both BaF-G133/Daxx#3 and/Daxx#6 cells was comparable to that in BaF-G133 cells (data not shown). Therefore, we assumed that Daxx does not participate in the modulation of the activation steps for STAT3 and ERK/MAPK signaling pathways.

We have previously shown that the DNA-binding domain of STAT3 (320–493) interacts with Daxx [16]; therefore, we next examined whether a reduction of Daxx expression affects the DNA-binding activity of STAT3. We introduced siControl or siDaxx into BaF-G133 cells. Cells were washed, starved for 12 h and stimulated with G-CSF for 10 and 30 min. As shown in Fig. 3B, G-CSF-induced STAT3 binding to its consensus oligonucleotide was clearly enhanced by siDaxx treatment, suggesting that Daxx has an inhibitory effect on the DNA-binding activity of STAT3. To investigate the effects of Daxx on the DNA-binding activity of STAT3 in the context of chromatin structure, we performed chromatin immunoprecipitation analysis on the STAT3-binding site in the 5′ region of the *JunB* gene (Fig. 3C). The STAT3-binding site was amplified by PCR in all of the sheared DNA samples (top, indicated as "Input"). In addition, this region was amplified by PCR from the anti-STAT3 immunoprecipitates obtained from G-CSF-stimulated cells (middle, lane 2), but not from control Ig immunoprecipitates (bottom), indicating that STAT3 activated by G-CSF bound to this element. Importantly, siDaxx transfection enhanced this binding (middle, lane 4). These findings indicate that Daxx also inhibits DNA-binding activity of STAT3 in chromatin.

To further delineate the functional relevance of Daxx in STAT3 regulation, we examined the status of STAT3-target gene expression in BaF-G133 cells. Either siControl- or siDaxx-transfected cells were treated with G-CSF for 30 min, followed by RNA extraction, reverse transcription and RT-PCR analysis using mouse *Socs3*-specific primers. The *Socs3* mRNA levels were normalized against *Actb*. As shown in Fig. 3D, *Socs3* was induced 6-fold with G-CSF treatment in the control cells and *Socs3* was induced by almost 13-fold in the siDaxx-transfected cells, suggesting that the siDaxx-transfected cells have enhanced expression of STAT3-target genes. Consistent with these observations, knockdown of Daxx in BaF-G133 cells also resulted in enhanced induction of other known STAT3-target genes, *JunB* and *Pim2* (Fig. 3E).

Daxx is involved in the regulation of Bcl2 mRNA and protein levels

Dimerization of G-CSFR-gp130 chimeric receptors in BaF-G133 cells transduces anti-apoptotic signal through the induction of *Bcl2* [32]. Thus, we next examined the effects of Daxx knockdown on the mRNA levels of *Bcl2* family genes. After washing with IL-3-free medium, BaF-G133 cells were stimulated with G-CSF and mRNA levels were analyzed by semi-quantitative RT-PCR, as indicated in Fig. 4A. In control siRNA-transfected cells, G-CSF treatment induced the upregulation of *Bcl2* mRNA levels, but not of *Bcl2l1*, which encodes the Bcl-x protein. The mRNA level of pro-apoptotic *Bax* was unaffected by G-CSF. Notably, knockdown of Daxx increased the basal level of *Bcl2* mRNA, indicating that Daxx regulates transcription factors involved in *Bcl2* expression other than activated STAT3. Reciprocally, BaF-G133 cells over-expressing Daxx exhibited decreased *Bcl2* mRNA levels regardless of G-CSF stimulation (Fig. 4B). In addition, we introduced siDaxx into BaF-G133 to knockdown endogenous Daxx and found an increase in protein levels of Bcl2 in the absence of G-CSF (Fig. 4C). We also prepared cell extracts from BaF-G133 or BaF-G133/Daxx#3 cells and analyzed endogenous protein levels of Bcl2 and Bax by western blotting. As shown in Fig. 4D, reduced expression of Bcl2 was observed in BaF-G133/Daxx#3 cells in G-CSF-treated conditions and also in non-G-CSF-treated conditions. Protein levels of Bax, however, were unaltered by G-CSF stimulation or Daxx expression. Interestingly, we also found that a decrease of Daxx protein preceded the up-regulation of Bcl2 after G-CSF-stimulation. Collectively, these data indicate that Daxx rather specifically regulates *Bcl2* expression at the mRNA level under both basement and G-CSF-stimulated conditions.

It has been shown that the cyclic AMP response element (CRE) is a major positive regulatory site in the *Bcl2* promoter in B-cells and that mutation of the CRE abolishes the binding of CREB/ATF and CREB-Binding Protein (CBP) transcription factors

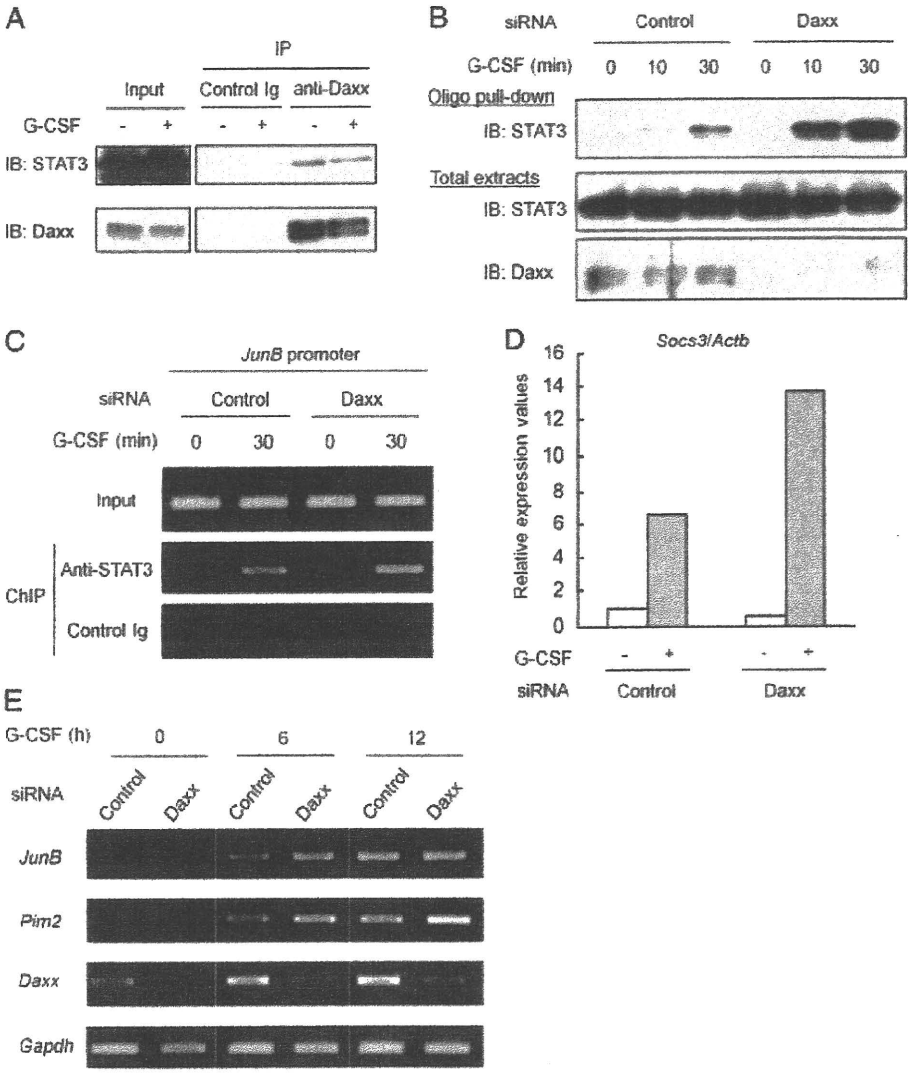

Figure 3. Daxx interacts with STAT3 and inhibits its activity. (A) BaF-G133 cells (5×10^7 cells) were stimulated with G-CSF (30 ng/ml) for 30 min. The cells were lysed, immunoprecipitated with control IgG or anti-Daxx antibody and subjected to western blot analysis of STAT3 and Daxx. An aliquot of total cell extract (input) was also analyzed. (B) BaF-G133 cells (2×10^6 cells) were treated with control siRNA or Daxx siRNA, and cells were stimulated with G-CSF (30 ng/ml) for the indicated periods. Cell extracts were prepared and subjected to pull-down experiments using the immobilized STAT3 consensus oligonucleotide-sepharose conjugate to evaluate DNA binding activity of STAT3. The precipitates and an aliquot of total cell extract were subjected to western blot analysis of STAT3. (C) BaF-G133 cells (4×10^6 cells) were treated with control siRNA or Daxx siRNA and cells were stimulated with G-CSF (30 ng/ml) for the indicated periods. Samples for ChIP were prepared as described in the *Materials and methods* section. STAT3-DNA binding complexes were immunoprecipitated with the anti-STAT3 antibody or with control IgG. The immunoprecipitated DNA was eluted and subjected to PCR. (D) BaF-G133 cells were treated with control or Daxx siRNA and cells were stimulated with G-CSF (30 ng/mL) for 30 min. Total RNA samples isolated from these cells were subjected to quantitative RT-PCR analysis using *Socs3* or *Actb* primers. Data represent the levels of *Socs3* mRNA normalized to that of an *Actb* internal control and are expressed relative to the value of control siRNA-treated samples without G-CSF-stimulation. Results are representative of three independent, duplicate experiments. (E) BaF-G133 cells were treated with control or Daxx siRNA and cells were stimulated with G-CSF (30 ng/ml) for the indicated periods. Total RNA samples isolated from these cells were subjected to semi quantitative RT-PCR analysis using *JunB*, *Pim2*, *Daxx* or *Gapdh* primers. Data in (A), (C) and (E) are representative of three independent experiments; (B) is representative of two independent experiments.

to the *Bcl2* promoter and greatly diminishes the binding of NF-κB factors [34]. Because Daxx can interact with RelA [10] and RelB [11], two members of the NF-κB family of transcription factors, as well as CBP [35], we next examined the binding of these proteins to the region of the *Bcl2* promoter containing the CRE site. The ChIP assays were performed with G-CSF-treated BaF-G133 and BaF-G133/Daxx#3 cells, and an anti-rabbit IgG was used as a nonspecific immunoprecipitation control. The results demonstrated that in BaF-G133 cells, RelA and CBP, but not RelB, binds to the CRE site (Fig. 4E). In addition, a substantial decrease in the binding of RelA and CBP was observed in the BaF-G133/Daxx#3 cells (Fig. 4E). These results indicated that Daxx negatively regulates RelA and CBP binding to the Bcl2 promoter in BaF-G133 cells.

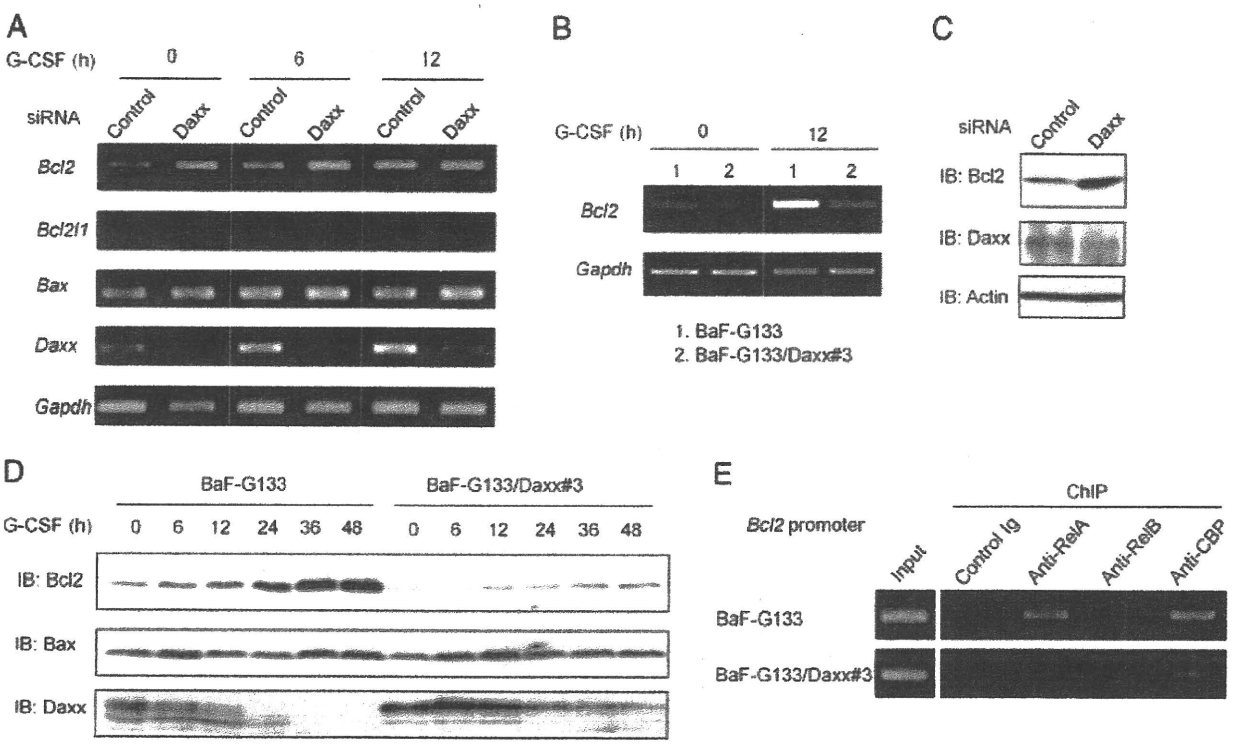

Figure 4. Daxx suppresses Bcl2 mRNA and protein levels. (A) cDNA samples, prepared as described in Fig. 3E, were subjected to semi quantitative analysis using *Bcl2*, *Bcl2l1* and *Bax* primers. (B) BaF-G133 or BaF-G133/Daxx#3 cells were treated with G-CSF at 30 ng/mL for 12 h. Total RNA was then extracted and subjected to RT-PCR analysis. (C) BaF-G133 cells were transfected with control siRNA or Daxx siRNA and endogenous Bcl2 protein was detected by western blot analysis. (D) BaF-G133 and BaF-G133/Daxx#3 cells were treated with 30 ng/mL G-CSF for the indicated times. Protein levels of Bcl2, Bax and Daxx in cells were detected by western blot analysis. (E) BaF-G133 or BaF-G133/Daxx#3 cells (4×10^6 cells) were stimulated with G-CSF (30 ng/mL) for 6 h. Samples for ChIP were prepared as described in the *Materials and methods* section. Transcription factor-DNA binding complexes were immunoprecipitated with indicated antibodies or with control IgG. The immunoprecipitated DNA was analyzed by PCR using primers that amplified a 100-bp product that includes the CRE site in the *Bcl2* promoter. Data in this figure are representative of three independent experiments.

Over-expression of Bcl2 represses Daxx-mediated cell death

We then analyzed whether Daxx-mediated cell death of BaF-G133 cells was repressed by over-expression of Bcl2. In G-CSF-treated conditions, over-expression of Bcl2 in BaF-G133/Daxx#3 cells decreased LDH leakage to a level comparable with that observed in control BaF-G133 cells (Fig. 5A, left and 5B). Treatment with HA14-1, a small-molecule Bcl2 inhibitor [36], decreased cell viability in a dose-dependent manner in G-CSF-treated BaF-G133 cells (Fig. 5C), confirming that Bcl2 function contributes to gp130-mediated survival of this cell line. These data indicate that the Daxx-mediated increase in cell death is due, at least in part, to changes in Bcl2 expression in G-CSF-treated BaF-G133 cells.

Discussion

Our present manipulation of Daxx expression has revealed that Daxx negatively regulates gp130-mediated signals. We here proposed and discussed two possible mechanisms concerning to STAT3 and Bcl2. Daxx constitutively interacted with STAT3, resulting in the impaired binding of STAT3 to its consensus DNA sequence in chromatin. In addition, Daxx preferentially down-regulated *Bcl2* expression at the mRNA level. These cellular modifications mediated by Daxx are likely to suppress gp130-mediated cell proliferation and survival.

The involvement of STAT3 in IL-6/gp130-mediated growth responses has been indicated by many investigators. For example, the G1 to S phase progression of cell cycle was shown to be a STAT3-dependent process [33]. In BaF-G133 cells, G-CSF-treatment was reported to induce dimerization of G-CSFR/gp130 chimeric receptors causing activation of STAT3 as well as STAT3-dependent cell growth [32]. In lymphocytes, STAT3 activation is reported to be responsible for IL-6-dpendent T-cell proliferation [29] and for normal early B-cell development [31]. With regard to this gp130-mediated STAT3 function, we here showed constitutive interactions between endogenous Daxx and STAT3. Of importance, our data clearly indicated that these interactions gave rise to a decrease in the DNA-binding activity of STAT3 rather than that in the activation steps of STAT3. Our previous report telling that the DNA-binding domain of STAT3 (320–493) was a major domain to interact with Daxx [16] might explain the inhibition of STAT3 transcription by Daxx.

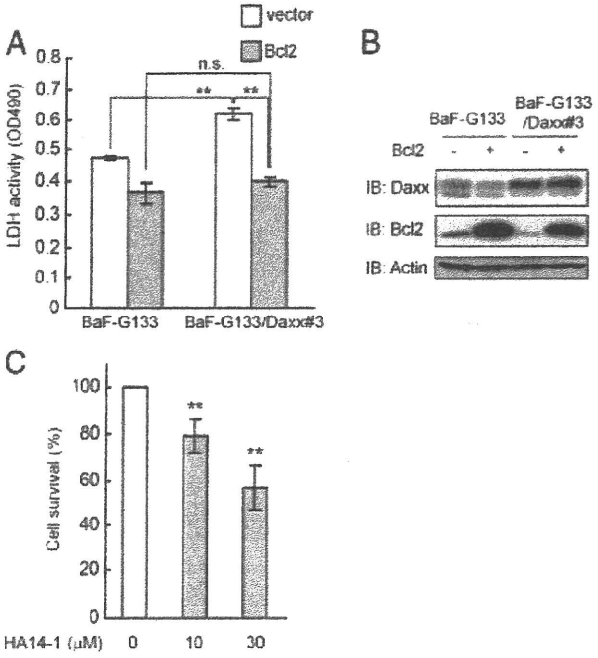

Figure 5. Over-expression of Bcl2 repressed Daxx-mediated cell death. (A) BaF-G133 or BaF-G133/Daxx#3 cells were transfected with empty plasmid or Bcl2 expression plasmid. After treatment with G-CSF (30 ng/mL, left) for 48 h, LDH activities in culture supernatants were measured. Results are presented as OD at 490 nm (mean ± SD, $n = 3$; $^{**}p<0.01$ and n.s., not significant). (B) Transient over-expression of Bcl2 in BaF-G133 or BaF-G133/Daxx#3 cells was validated by western blot analysis of Daxx, Bcl2 and β-actin. Data are representative of three independent experiments. (C) BaF-133 cells were plated in a 96-well plate in the presence of G-CSF (30 ng/mL) without or with the indicated concentrations of the small-molecule Bcl2 inhibitor, HA14-1. Twenty-four hours after treatment, cell number was determined by the WST8 assay. The value obtained for DMSO-treated (0 μM) cells was set as 100% survival. Data show mean ± SD ($n = 3$). $^{**}p<0.01$ (Student's t-test).

Although Daxx negatively regulated gp130-mediated *Bcl2* mRNA induction, it also reduced basal level of *Bcl2* expression at the mRNA level. This is likely to suggest that Daxx must have further targets for repression, in addition to activated STAT3. In this regard, we first considered ETS1 to be a candidate, because *Bcl2* is induced by over-expression of ETS1 [7]. However, we could not detect any *Ets1* mRNA expression in BaF-G133 cells (data not shown), indicating that ETS1 is not involved in the Bcl2 expression in those cells. *Bcl2* is also a well-known anti-apoptotic target gene of NF-κB. Daxx can interact with RelA [10], RelB [11] and CBP [35], we therefore assessed the effect of Daxx over-expression on Rel and CBP binding to the *Bcl2* promoter. Our ChIP experiments using the primers amplifying the Bcl2 promoter region containing the CRE clearly indicated that Daxx negatively regulates RelA and CBP in BaF-G133 cells. In addition, our experiments using a Bcl2-specific inhibitor indicated that gp130-mediated Bcl2 expression is indeed involved in the maintenance of cell survival and that Daxx specifically inhibits the *Bcl2* expression. During apoptosis of lymphocytes, an inverse correlation of Daxx and Bcl2 expression levels has been suggested to be important. For example, gene expression profiling of interferon-β-treated progenitor B cells revealed enhanced Daxx expression and nuclear accumulation, with subsequent down-regulation of *Bcl2*, followed by apoptosis [3]. Another report said that certain mantle cell lymphomas have markedly decreased levels of *Daxx* expression and exhibit over-expression of *Bcl2* and *Bcl2l1* [37]. It has also been reported that ectopic over-expression of Daxx down-regulates *Bcl2* in malignant lymphocyte Jurkat T-cells and sensitizes cells to the apoptosis-inducing effect of chemotherapeutic agents [38]. These findings and our results support the idea that Daxx participates in repression, especially that of *Bcl2* gene expression and thereby sensitizes cell death.

As described above, Daxx inhibited gp130-mediated cell growth and survival in BaF-G133 cells. In a case of IL-3 signals, which mainly utilize STAT5 [39–41], manipulation of Daxx expression failed to modify their growth and/or survival (data not shown). This different involvement of Daxx may come from the difference in activated STAT proteins between gp130- and IL-3-mediated signaling. In accordance with this notion, we could not detect the specific interactions between Daxx and STAT5 in our co-immunoprecipitation experiments (data not shown). These observations indicate that Daxx preferentially interacts with and inhibits STAT3 rather than STAT5.

The functions of Daxx are related to its protein level. It has been reported that the peptidyl–prolyl isomerase, Pin1, inhibits Daxx-mediated apoptosis by inducing Daxx ubiquitination and degradation [42], and that the BTB domain-containing speckle-type POZ protein/Cul3 ubiquitin ligase complex inhibits the transcriptional repression function of Daxx by mediating the proteasome-dependent degradation of Daxx [43]. Furthermore, Mdm2 and Hausp regulate Daxx functions by controlling Daxx ubiquitination and stability [44]. Interestingly, we found that gp130-mediated up-regulation of Bcl2 is accompanied by a reduction in the level of endogenous Daxx protein. This reduction of Daxx protein may be regulated by the above factors and may be an important process in the 'de-repression' mechanism for the regulation of both STAT3 activity and Bcl2 expression, although the details of this are still unclear.

G-CSF is a common inducer of the release of hematopoietic progenitor cells (HPC) from the bone marrow into the peripheral blood [45]. One of the molecular mechanisms underlying this action of G-CSF has been implicated to involve the phosphorylation of JAK1/STAT3 pathway [46]. Daxx has been reported to be expressed in HPC [47]. Therefore, it is possible to speculate that Daxx could also influence G-CSF-mediated mobilization of HPC and the further study will be required to clarify this point.

In summary, we suggest that Daxx has two functional roles corresponding to cell death regulation: STAT3 repression and down-regulation of Bcl2. Our results suggest that the ability of Daxx to repress transcription is relevant to its ability to sensitize cell death. In addition, our finding that STAT3 function can be modulated by Daxx will provide insight into the regulation of various cellular events, malignancies and autoimmune diseases in which STAT3 plays critical roles.

Materials and methods

Cell culture

BaF-G133 cells were a kind gift from Dr. Toshio Hirano (Osaka University, Osaka, Japan) and have been described [32]. BaF-G133 cells are derived from an IL-3-dependent mouse pro-B cell line, BaF3, and were maintained in RPMI 1640 medium supplemented with 10% FBS (Trace Biosystems, Sydney, Australia), 10% conditioned medium from WEHI-3B cells as a source of IL-3, 100 U/mL penicillin and 100 μg/mL streptomycin. BaF-G133 cells stably express the chimeric receptor G133, which is composed of the extracellular domain of the G-CSF receptor and the transmembrane and cytoplasmic domains of gp130 (truncation of gp130 occurs 133 amino acids from the transmembrane domain). G133 contains gp130 Tyr767, which is required for STAT3 activation and STAT3 is essential for both gp130-mediated cell survival [32] and gp130-mediated cell-cycle transition [33]. To establish Daxx transfectants, 20 μg of human Daxx expression vector (pCDNA3–FLAG–Daxx) was co-transfected with 2 μg of pMIK–Hyg into BaF-G133 cells by electroporation. Daxx transfectants were selected using 200 μg/mL hygromycin. Independent clones were established using a limiting dilution procedure. Expression levels of Daxx were analyzed by western blotting. Human G-CSF was kindly provided by Chugai Pharmaceutics (Tokyo, Japan).

siRNA Experiments

Mouse Daxx stealth siRNA was purchased from Invitrogen (Carlsbad, CA, USA). The sequence of the mouse Daxx siRNA was 5′-AAGUAGAAGAGACCAUGCCUGCUCC-3′. Stealth siRNA negative control medium GC (Invitrogen) was used as a negative control. BaF-G133 cells were transfected using a Nucleofector (Amaxa Biosystems, Cologne, Germany). Cells were transfected with 200 pmol siRNA in Nucleofector solution V using program X-001. Immediately following transfection medium was added to the BaF-G133 cells, which were then plated in 6-well tissue culture plates and incubated overnight. Cells were collected the following day and analyzed for protein expression by western blotting.

Proliferation assays

Cell proliferation was determined using the Cell Counting Kit-8 (Dojindo, Kumamoto, Japan) according to the manufacturer's instructions. Briefly, cells were plated in a 96-well plate at 1×10^4 cells/well and left untreated or were treated with G-CSF at concentrations indicated in figures. Ten microliters of WST-8 mixture was then added to each well, and the plates were incubated at 37°C in 5% CO_2 for 4 h. The absorbance of each well was then measured on a microplate reader at 450 nm. All assays were performed in triplicate and repeated at least three times. To investigate the role of Bcl2 in G-CSF-induced cell growth, a small-molecule Bcl2 inhibitor, HA14-1 (Calbiochem, San Diego, CA, USA) was used.

Immunoprecipitation, STAT3 DNA-binding assay and western blotting

The immunoprecipitation and western blotting assays were performed as described previously [48]. The DNA-binding activity of STAT3 in cell extracts was measured using an immobilized STAT3 consensus oligonucleotide–Sepharose conjugate (Santa Cruz Biotechnology, Santa Cruz, CA, USA) as described previously [49]. The immunoprecipitates or consensus oligo-binding proteins from cell lysates were resolved by SDS-PAGE and transferred to PVDF membranes (PerkinElmer, Boston, MA, USA). The membranes were then immunoblotted with the different primary antibodies. Immunoreactive proteins were visualized using an enhanced chemiluminescence detection system (Millipore, Bedford, MA, USA). Antibodies used in this study were: anti-Daxx (sc-7152), anti-STAT3 (sc-482) and anti-Bcl2 (sc-7382) from Santa Cruz Biotechnology, anti-Bax (♯2772) from Cell Signaling technology (Beverly, MA, USA) and anti-Actin (A1978) from Sigma.

Cell cycle analysis

BaF-G133 (2×10^5) cells were IL-3-starved for 12 h and then treated with 30 ng/mL G-CSF. Cells were then washed once with ice-cold PBS, suspended with 100 μL of PBS and then fixed by the addition of 900 μL of ethanol. Cells were incubated at −20°C for 20 min, pelleted, resuspended with 300 μL of staining buffer (1 mg/mL RNase, 20 μg/mL propidium iodide, 0.01% NP-40 in PBS) and incubated at 37°C for 20 min. The DNA content of nuclei was analyzed using an FACSCalibur and CellQuest software (BD Biosciences, San Jose, CA, USA).

LDH release assay

Cytotoxicity was determined by measuring the release of LDH using an LDH Cytotoxicity Detection Kit (Takara, Otsu, Japan) according to the manufacturer's instructions. The reaction was initiated by mixing 50 μL of cell-free supernatant with a potassium phosphate buffer containing NADH and sodium pyruvate to a final volume of 100 μL in a 96-well plate. The absorbance of the sample was read at 490 nm. Data were normalized to the activity of LDH released from control cells (100%) and are expressed as a percentage of the control value.

Table 1. RT-PCR primers used in this study

Target	Forward primer (5′–3′)	Reverse primer (5′–3′)
Bax	TGCAGAGGATGATTGCTGAC	GATCAGCTCGGGCACTTTAG
Bcl2	GTCGCTACCGTCGTCACTTC	ACAGCCAGGAGAAATCAAAC
Bcl2l1	TAGGACTGAGGCCCCAGAAG	CAGTCATGCCCGTCAGGAAC
Daxx	CCCATGGCCACCGATGACAGCAT	AGGGTTAGGGCCCGACGCCTCACT
Gapdh	CAGTAGAGGCAGGGATGATGTTC	GAAATCCCATCACCATCTTCCAGG
JunB	CAGGCAGCTACTTTTCGGGTC	AAGGGTGGTGCATGTGGGAGG
Pim2	AGCACCTCCTCCATGTTGAC	ATGGCCACCTGACGTCTATC

Chromatin immunoprecipitation

Cells were treated with 1% formaldehyde for 20 min to crosslink proteins to DNA. Formaldehyde was neutralized for 5 min by the addition of glycine to 125 mM. Cells were washed twice with cold PBS. Cells were resuspended in lysis buffer (1% SDS, 10 mM EDTA, 50 mM Tris pH 8.0) and incubated at 4°C for 10 min. The suspension was then sonicated with five 10 s pulses and then clarified by centrifugation for 10 min in a microcentrifuge. The supernatant was diluted 10-fold with dilution buffer (1% Triton X-100, 0.1% sodium deoxycholate, 150 mM NaCl, 50 mM Tris-HCl at pH 8.0) to yield the solubilized chromatin solution. The resulting material was used for immunoprecipitation with anti-STAT3 (sc-482), anti-RelA (sc-372), anti-RelB (sc-226), anti-CBP (sc-369) from Santa Cruz Biotechnology or with rabbit IgG as a negative control. After overnight incubation with antibody, DNA-protein complexes were collected by the addition of 10 μL of salmon sperm DNA-protein A agarose (Upstate Biotechnology, Lake Placid, NY, USA) and incubated at 4°C with rotation for 2 h. Following immunoprecipitation, beads were washed in RIPA buffer (1% Triton X-100, 0.1% SDS, 0.1% sodium deoxycholate, 150 mM NaCl, 1 mM EDTA, 50 mM Tris-HCl at pH 8.0), followed by RIPA/500 mM NaCl, LiCl buffer (250 mM LiCl, 0.5% NP-40, 0.5% sodium deoxycholate, 1 mM EDTA, 10 mM Tris-HCl at pH 8.0), and finally, TE buffer. The immunoprecipitated complexes were eluted in a buffer containing 10 mM Tris pH 8.0, 300 mM NaCl, 5 mM EDTA, 0.5% SDS at 65°C for 6 h. The samples were then treated with proteinase K for 1 h, and DNA was purified by phenol/chloroform extraction and ethanol precipitation. Immunoprecipitates were analyzed by PCR. PCR primers were designed to amplify −454/−186 of the *JunB* promoter, as described previously [50] and to amplify −1560/−1461 of the *Bcl2* promoter region containing the CRE as follows: the forward primer was 5′-GCTCAGAGGAGGGCTTTCTT-3′ and the reverse primer was 5′-GGCCCGGCCTCTTACTTC-3′. PCR products were electrophoresed on agarose gels and visualized by EtBr staining.

RNA extraction and RT-PCR analysis

Total RNA was extracted from BaF-G133 cells using TRI Reagent (Molecular Research Center, Cincinnati, OH, USA). First-strand cDNA was synthesized from 1 μg of total RNA with Revertra Ace reverse transcriptase (TOYOBO, Osaka, Japan) using random nonamers. The cDNA was the template for PCR using Gene Taq polymerase (Wako Pure Chemical, Osaka, Japan) according to the manufacturer's instructions. PCR products were electrophoresed on agarose gels and visualized by EtBr staining. The primer pairs used in this study were listed in Table 1. Quantitative real-time PCR analysis of *Socs3* mRNA transcripts was carried out using the assay-on-demand™ gene-specific fluorescently labeled TaqMan MGB probe in an ABI Prism 7000 sequence detection system.

Statistical analysis

Statistical evaluation of differences between populations was determined using Student's unpaired, two-tailed *t* test. Results shown are the means and standard deviations.

Acknowledgements: We thank T. Hirano for the gift of the BaF-G133 cell line. We also thank R. Kitamoto, M. Nakajima and S. Kamitani for technical assistance. This work was supported in part by a Grant-in-Aid from the Japanese Ministry of Education, Science, Sports and Culture, by the Northern Advancement Center for Science and Technology, and by The Akiyama Foundation.

Conflict of interest: The authors declare no financial or commercial conflict of interest.

References

1 **Salomoni, P. and Khelifi, A. F.**, Daxx: death or survival protein? *Trends Cell Biol.* 2006. 16: 97–104.

2 **Michaelson, J. S.**, The Daxx enigma. *Apoptosis* 2000. 5: 217–220.

3 **Gongora, R., Stephan, R. P., Zhang, Z. and Cooper, M. D.**, An essential role for Daxx in the inhibition of B lymphopoiesis by type I interferons. *Immunity* 2001. 14: 727–737.

4 **Zhong, S., Salomoni, P., Ronchetti, S., Guo, A., Ruggero, D. and Pandolfi, P. P.,** Promyelocytic leukemia protein (PML) and Daxx participate in a novel nuclear pathway for apoptosis. *J. Exp. Med.* 2000. **191**: 631–640.

5 **Salomoni, P., Guernah, I. and Pandolfi, P. P.,** The PML-nuclear body associated protein Daxx regulates the cellular response to CD40. *Cell Death Differ.* 2006. **13**: 672–675.

6 **Leal-Sanchez, J., Couzinet, A., Rossin, A., Abdel-Sater, F., Chakrabandhu, K., Luci, C., Anjuere, F. *et al.*,** Requirement for Daxx in mature T-cell proliferation and activation. *Cell Death Differ.* 2007. **14**: 795–806.

7 **Li, R., Pei, H., Watson, D. K. and Papas, T. S.,** EAP1/Daxx interacts with ETS1 and represses transcriptional activation of ETS1 target genes. *Oncogene* 2000. **19**: 745–753.

8 **Emelyanov, A. V., Kovac, C. R., Sepulveda, M. A. and Birshtein, B. K.,** The interaction of Pax5 (BSAP) with Daxx can result in transcriptional activation in B cells. *J. Biol. Chem.* 2002. **277**: 11156–11164.

9 **Lin, D. Y., Lai, M. Z., Ann, D. K. and Shih, H. M.,** Promyelocytic leukemia protein (PML) functions as a glucocorticoid receptor co-activator by sequestering Daxx to the PML oncogenic domains (PODs) to enhance its transactivation potential. *J. Biol. Chem.* 2003. **278**: 15958–15965.

10 **Park, J., Lee, J. H., La, M., Jang, M. J., Chae, G. W., Kim, S. B., Tak, H. *et al.*,** Inhibition of NF-kappaB acetylation and its transcriptional activity by Daxx. *J. Mol. Biol.* 2007. **368**: 388–397.

11 **Croxton, R., Puto, L. A., de Belle, I., Thomas, M., Torii, S., Hanaii, F., Cuddy, M. *et al.*,** Daxx represses expression of a subset of antiapoptotic genes regulated by nuclear factor-kappaB. *Cancer Res.* 2006. **66**: 9026–9035.

12 **Tzeng, S. L., Cheng, Y. W., Li, C. H., Lin, Y. S., Hsu, H. C. and Kang, J. J.,** Physiological and functional interactions between Tcf4 and Daxx in colon cancer cells. *J. Biol. Chem.* 2006. **281**: 15405–15411.

13 **Chang, C. C., Lin, D. Y., Fang, H. I., Chen, R. H. and Shih, H. M.,** Daxx mediates the small ubiquitin-like modifier-dependent transcriptional repression of Smad4. *J. Biol. Chem.* 2005. **280**: 10164–10173.

14 **Wethkamp, N. and Klempnauer, K. H.,** Daxx is a transcriptional repressor of CCAAT/enhancer-binding protein beta. *J. Biol. Chem.* 2009. **284**: 28783–28794.

15 **Meloni, A., Fiorillo, E., Corda, D., Incani, F., Serra, M. L., Contini, A., Cao, A. *et al.*,** DAXX is a new AIRE-interacting protein. *J. Biol. Chem.* 2010. **285**: 13012–13021.

16 **Muromoto, R., Nakao, K., Watanabe, T., Sato, N., Sekine, Y., Sugiyama, K., Oritani, K. *et al.*,** Physical and functional interactions between Daxx and STAT3. *Oncogene* 2006. **25**: 2131–2136.

17 **Hollenbach, A. D., McPherson, C. J., Mientjes, E. J., Iyengar, R. and Grosveld, G.,** Daxx and histone deacetylase II associate with chromatin through an interaction with core histones and the chromatin-associated protein Dek. *J. Cell Sci.* 2002. **115**: 3319–3330.

18 **Michaelson, J. S., Bader, D., Kuo, F., Kozak, C. and Leder, P.,** Loss of Daxx, a promiscuously interacting protein, results in extensive apoptosis in early mouse development. *Genes Dev.* 1999. **13**: 1918–1923.

19 **Puto, L. A. and Reed, J. C.,** Daxx represses RelB target promoters *via* DNA methyltransferase recruitment and DNA hypermethylation. *Genes Dev.* 2008. **22**: 998–1010.

20 **Muromoto, R., Sugiyama, K., Takachi, A., Imoto, S., Sato, N., Yamamoto, T., Oritani, K. *et al.*,** Physical and functional interactions between Daxx and DNA methyltransferase 1-associated protein, DMAP1. *J. Immunol.* 2004. **172**: 2985–2993.

21 **Xue, Y., Gibbons, R., Yan, Z., Yang, D., McDowell, T. L., Sechi, S., Qin, J. *et al.*,** The ATRX syndrome protein forms a chromatin-remodeling complex with Daxx and localizes in promyelocytic leukemia nuclear bodies. *Proc. Natl. Acad. Sci. USA* 2003. **100**: 10635–10640.

22 **Tang, J., Wu, S., Liu, H., Stratt, R., Barak, O. G., Shiekhattar, R., Picketts, D. J. *et al.*,** A novel transcription regulatory complex containing death domain-associated protein and the ATR-X syndrome protein. *J. Biol. Chem.* 2004. **279**: 20369–20377.

23 **Hirano, T., Nakajima, K. and Hibi, M.,** Signaling mechanisms through gp130: a model of the cytokine system. *Cytokine Growth Factor Rev.* 1997. **8**: 241–252.

24 **Darnell, J. E., Jr.,** STATs and gene regulation. *Science* 1997. **277**: 1630–1635.

25 **Taga, T. and Kishimoto, T.,** Gp130 and the interleukin-6 family of cytokines. *Annu. Rev. Immunol.* 1997. **15**: 797–819.

26 **Hankey, P. A.,** Regulation of hematopoietic cell development and function by Stat3. *Front. Biosci.* 2009. **14**: 5273–5290.

27 **Yu, H., Pardoll, D. and Jove, R.,** STATs in cancer inflammation and immunity: a leading role for STAT3. *Nat. Rev. Cancer* 2009. **9**: 798–809.

28 **Minegishi, Y.,** Hyper-IgE syndrome. *Curr. Opin. Immunol.* 2009. **21**: 487–492.

29 **Takeda, K., Kaisho, T., Yoshida, N., Takeda, J., Kishimoto, T. and Akira, S.,** Stat3 activation is responsible for IL-6-dependent T cell proliferation through preventing apoptosis: generation and characterization of T cell-specific Stat3-deficient mice. *J. Immunol* 1998. **161**: 4652–4660.

30 **Owaki, T., Asakawa, M., Morishima, N., Mizoguchi, I., Fukai, F., Takeda, K., Mizuguchi, J. *et al.*,** STAT3 is indispensable to IL-27-mediated cell proliferation but not to IL-27-induced Th1 differentiation and suppression of proinflammatory cytokine production. *J. Immunol.* 2008. **180**: 2903–2911.

31 **Chou, W. C., Levy, D. E. and Lee, C. K.,** STAT3 positively regulates an early step in B-cell development. *Blood* 2006. **108**: 3005–3011.

32 **Fukada, T., Hibi, M., Yamanaka, Y., Takahashi-Tezuka, M., Fujitani, Y., Yamaguchi, T., Nakajima, K. *et al.*,** Two signals are necessary for cell proliferation induced by a cytokine receptor gp130: involvement of STAT3 in anti-apoptosis. *Immunity* 1996. **5**: 449–460.

33 **Fukada, T., Ohtani, T., Yoshida, Y., Shirogane, T., Nishida, K., Nakajima, K., Hibi, M. *et al.*,** STAT3 orchestrates contradictory signals in cytokine-induced G1 to S cell-cycle transition. *EMBO J.* 1998. **17**: 6670–6677.

34 **Xiang, H., Wang, J. and Boxer, L. M.,** Role of the cyclic AMP response element in the bcl-2 promoter in the regulation of endogenous Bcl-2 expression and apoptosis in murine B cells. *Mol. Cell Biol.* 2006. **26**: 8599–8606.

35 **Kuo, H. Y., Chang, C. C., Jeng, J. C., Hu, H. M., Lin, D. Y., Maul, G. G., Kwok, R. P. *et al.*,** SUMO modification negatively modulates the transcriptional activity of CREB-binding protein *via* the recruitment of Daxx. *Proc. Natl. Acad. Sci. USA* 2005. **102**: 16973–16978.

36 **Wang, J. L., Liu, D., Zhang, Z. J., Shan, S., Han, X., Srinivasula, S. M., Croce, C. M. *et al.*,** Structure-based discovery of an organic compound that binds Bcl-2 protein and induces apoptosis of tumor cells. *Proc. Natl. Acad. Sci. USA* 2000. **97**: 7124–7129.

37 **Hofmann, W. K., de Vos, S., Tsukasaki, K., Wachsman, W., Pinkus, G. S., Said, J. W. and Koeffler, H. P.,** Altered apoptosis pathways in mantle cell lymphoma detected by oligonucleotide microarray. *Blood* 2001. **98**: 787–794.

38 **Boehrer, S., Nowak, D., Kukoc-Zivojnov, N., Hochmuth, S., Kim, S. Z., Hoelzer, D., Mitrou, P. S. *et al.*,** Expression of Daxx sensitizes Jurkat T-cells to the apoptosis-inducing effect of chemotherapeutic agents. *Pharmacol. Res.* 2005. **51**: 367–374.

39 **Mui, A. L., Wakao, H., Kinoshita, T., Kitamura, T. and Miyajima, A.,** Suppression of interleukin-3-induced gene expression by a C-terminal truncated Stat5: role of Stat5 in proliferation. *EMBO J.* 1996. **15**: 2425–2433.

40 **Dumon, S., Santos, S. C., Debierre-Grockiego, F., Gouilleux-Gruart, V., Cocault, L., Boucheron, C., Mollat, P. *et al.*,** IL-3 dependent regulation of

Bcl-xL gene expression by STAT5 in a bone marrow derived cell line. *Oncogene* 1999. 18: 4191–4199.

41 **Rosa Santos, S. C., Dumon, S., Mayeux, P., Gisselbrecht, S. and Gouilleux, F.,** Cooperation between STAT5 and phosphatidylinositol 3-kinase in the IL-3-dependent survival of a bone marrow derived cell line. *Oncogene* 2000. 19: 1164–1172.

42 **Ryo, A., Hirai, A., Nishi, M., Liou, Y. C., Perrem, K., Lin, S. C., Hirano, H. *et al.*,** A suppressive role of the prolyl isomerase Pin1 in cellular apoptosis mediated by the death-associated protein Daxx. *J. Biol. Chem.* 2007. 282: 36671–36681.

43 **Kwon, J. E., La, M., Oh, K. H., Oh, Y. M., Kim, G. R., Seol, J. H., Baek, S. H. *et al.*,** BTB domain-containing speckle-type POZ protein (SPOP) serves as an adaptor of Daxx for ubiquitination by Cul3-based ubiquitin ligase. *J. Biol. Chem.* 2006. 281: 12664–12672.

44 **Tang, J., Qu, L., Pang, M. and Yang, X.,** Daxx is reciprocally regulated by Mdm2 and Hausp. *Biochem. Biophys. Res. Commun.* 2010. 393: 542–545.

45 **Cashen, A. F., Lazarus, H. M. and Devine, S. M.,** Mobilizing stem cells from normal donors: is it possible to improve upon G-CSF? *Bone Marrow Transplantation* 2007. 39: 577–588.

46 **Zhang, Y., Cheng, G., Yang, K., Fan, R., Xu, Z., Chen, L., Li, Q. *et al.*,** A novel function of granulocyte colony-stimulating factor in mobilization of human hematopoietic progenitor cells. *Immunol. Cell Biol.* 2009. 87: 428–432.

47 **Saffert, R. T., Penkert, R. R. and Kalejta, R. F.,** Cellular and viral control over the initial events of human cytomegalovirus experimental latency in CD34+cells. *J. Virol.* 2010. 84: 5594–5604.

48 **Matsuda, T., Yamamoto, T., Muraguchi, A. and Saatcioglu, F.,** Cross-talk between transforming growth factor-beta and estrogen receptor signaling through Smad3. *J. Biol. Chem.* 2001. 276: 42908–42914.

49 **Muromoto, R., Ikeda, O., Okabe, K., Togi, S., Kamitani, S., Fujimuro, M., Harada, S. *et al.*,** Epstein-Barr virus-derived EBNA2 regulates STAT3 activation. *Biochem. Biophys. Res. Commun.* 2009. 378: 439–443.

50 **Ezoe, S., Matsumura, I., Gale, K., Satoh, Y., Ishikawa, J., Mizuki, M., Takahashi, S. *et al.*,** GATA transcription factors inhibit cytokine-dependent growth and survival of a hematopoietic cell line through the inhibition of STAT3 activity. *J. Biol. Chem.* 2005. 280: 13163–13170.

Abbreviations: **Bcl2:** B-cell lymphoma 2 · **CRE:** cyclic AMP response element · **Daxx:** Death domain-associated protein · **HPC:** hematopoietic progenitor cells · **LDH:** Lactate dehydrogenase · **G-CSFR:** G-CSF receptor

Full correspondence: Dr. Tadashi Matsuda, Department of Immunology, Graduate School of Pharmaceutical Sciences, Hokkaido University, Kita-12 Nishi-6, Kita-Ku, Sapporo, 060-0812, Japan
Fax: +81-11-706-4990
e-mail: tmatsuda@pharm.hokudai.ac.jp

Received: 21/5/2010
Revised: 2/8/2010
Accepted: 2/9/2010
Accepted article online 21/9/2010

Rituximab, B-Lymphocyte Depletion, and Beta-Cell Function

TO THE EDITOR: Pescovitz et al. (Nov. 26 issue)[1] reported that the use of B-lymphocyte depletion therapy with rituximab was effective in preserving beta-cell function in patients with newly diagnosed type 1 diabetes who did not have severe infections. B cells may play a role in preventing infection in vivo by taking up a specific pathogen when it enters the bloodstream. This event is followed by the presentation of the specific antigen to T cells, which increases the level of T-cell response to better control overwhelming infection; this sequence of events does not occur in response to local infections. In addition, since studies of B-cell knockout in autoimmune mice with diabetes have shown that T-cell response to islet cells (insulitis) is minimal, even in the presence of efforts to prevent the development of diabetes,[2,3] it follows that the cessation of rituximab therapy may induce autoreactive T cells to attack pancreatic beta cells. Thus, it is important to watch for the complications of severe infections[4,5] and, in the long-term, for appropriate beta-cell function when using rituximab in the treatment of patients with newly diagnosed type 1 diabetes.

Seiho Nagafuchi, M.D., Ph.D.
Hitoshi Katsuta, M.D., Ph.D.
Kyushu University
Fukuoka, Japan
nagafuchi@shs.kyushu-u.ac.jp

Keizo Anzai, M.D., Ph.D.
Saga University
Saga, Japan

No potential conflict of interest relevant to this letter was reported.

1. Pescovitz MD, Greenbaum CJ, Krause-Steinrauf H, et al. Rituximab, B-lymphocyte depletion, and preservation of beta-cell function. N Engl J Med 2009;361:2143-52.
2. Akashi T, Nagafuchi S, Anzai K, et al. Direct evidence for the contribution of B cells to the progression of insulitis and the development of diabetes in non-obese diabetic mice. Int Immunol 1997;9:1159-64.
3. Kondo S, Iwata I, Anzai K, et al. Suppression of insulitis and diabetes in B cell-deficient mice treated with streptozocin: B cells are essential for TCR clonotype spreading of islet-infiltrating T cells. Int Immunol 2000;12:1075-83.
4. Barnadas MA, Roe E, Brunet S, et al. Therapy of paraneoplastic pemphigus with rituximab: a case report and review of literature. J Eur Acad Dermatol Venereol 2006;20:69-74.
5. Lutt JR, Pisculli ML, Weinblatt ME, Deodhar A, Winthrop KL. Severe nontuberculous mycobacterial infection in 2 patients receiving rituximab for refractory myositis. J Rheumatol 2008;35:1683-6.

THE AUTHORS REPLY: We agree with Nagafuchi and colleagues that when patients with newly diagnosed diabetes are treated with rituximab, long-term follow-up is essential to rule out increased rates of infection and other adverse events. We acknowledged the long-term risk of unknown adverse events in our article and for this reason recommended that the use of such therapy should be limited to carefully controlled studies. Although the potential for an augmented response at the time of reconstitution is reasonable, such an event did not occur in models of nonobese mice with diabetes that were given anti-CD20 treatment.[1,2] Furthermore, we found that the rate of C-peptide loss did not accelerate with recovery of B cells between 6 months and 1 year into our study. Consequently, such a concern was not supported by experimental evidence.

Mark D. Pescovitz, M.D.
Indiana University
Indianapolis, IN
mpescov@iupui.edu

Jay S. Skyler, M.D.
University of Miami
Miami, FL

Since publication of their article, the authors report no further potential conflict of interest.

1. Xiu Y, Wong CP, Bouaziz JD, et al. B lymphocyte depletion by CD20 monoclonal antibody prevents diabetes in nonobese diabetic mice despite isotype-specific differences in Fc gamma R effector functions. J Immunol 2008;180:2863-75.
2. Hu CY, Rodriguez-Pinto D, Du W, et al. Treatment with CD20-specific antibody prevents and reverses autoimmune diabetes in mice. J Clin Invest 2007;117:3857-67.

Reprinted from THE NEW ENGLAND JOURNAL OF MEDICINE
(ISSN 0028-4793) Vol. 362:761-761 (February 25, 2010).

Printed in the U.S.A. Fax: (781) 893-8103 www.nejm.org

Diabetol Int (2010) 1:49–59
DOI 10.1007/s13340-010-0005-8

ORIGINAL ARTICLE

Different effects of islet transplantation and Detemir treatment on the reversal of streptozotocin-induced diabetes associated with β-cell regeneration

Akari Inada · Oogi Inada · Hiroshi Fujii · Tomoyuki Akashi · Katsuo Sueishi · Atsushi Fukatsu · Seiho Nagafuchi

Received: 7 June 2010 / Accepted: 23 August 2010 / Published online: 2 November 2010

Abstract Here we examined whether new β-cell formation occurs when β cells face being severely destroyed and hyperglycemia is restored. Animals were made diabetic by a single i.p. injection of a high dose of streptozotocin, and blood glucose levels were kept in the normal range with twice-daily Detemir (long-acting human insulin analog) injection or islet transplantation for 10 weeks. Although Detemir injection could effectively reverse hyperglycemia and glycemic control was successful, there was no β-cell increase, new formation, or recovery of islet morphology in Detemir-treated mice. In contrast, β-cell regeneration was restored when hyperglycemia was reversed by islet transplantation. The number of β cells and islets was increased, and islet structure was greatly recovered. We further evaluated whether replication or new formation contributes to the recovery. Newly born β cells, as observed as scattered singlets-doublets of insulin-positive cells or clusters of less than 6 β cells across, were frequently seen in transplanted mice, suggesting that neogenesis of β cells was enhanced in transplanted mice. Ki67-positive islets were increased in transplanted mice, suggesting that β-cell proliferation is enhanced. Thus, this recovery involved both increased new formation and replication. Our results suggest that the effects of Detemir on pancreatic β cells were very different from those of islet transplantation and that islet transplantation could be a trigger for the induction of new formation and replication.

Keywords Islet regeneration · Diabetes · Islet transplantation · Organ injury

A. Inada (✉) · O. Inada
Section of Diabetes and Genes, Stem Cell Unit, Graduate School of Medical Sciences, Kyushu University, 3-1-1 Maidashi, Higashi-ku, Fukuoka 812-8582, Japan
e-mail: inadaa@bcell.med.kyushu-u.ac.jp

H. Fujii · K. Sueishi
Division of Pathophysiological and Experimental Pathology, Graduate School of Medical Sciences, Kyushu University, Fukuoka, Japan

T. Akashi
Medical Shimada Hospital, Fukuoka, Japan

A. Fukatsu
Department of Nephrology, Graduate School of Medicine, Kyoto University, Kyoto, Japan

S. Nagafuchi
Laboratory of Viral and Molecular Immunology of Diabetes, Department of Medical Science and Technology, Graduate School of Medical Sciences, Kyushu University, Fukuoka, Japan

Present Address:
K. Sueishi
National Hospital Organization Fukuoka-Higashi Medical Center, Fukuoka, Japan

Introduction

Vigorous studies have shown that pancreatic β-cells have the ability to adapt to physiological changes. To maintain glycemic levels, β-cell number/mass increases for (1) the normal growth after birth with body growth; (2) increased demand to compensate, such as pregnancy, chronic glucose infusion, obesity, and response to insulin resistance; and (3) tissue injury [1–9]. For new β-cell formation, two pathways are thought to exist, the replication of existing β cells and neogenesis from precursors [10]. Neogenesis,

insulin-positive cells budding from the ducts, has been reported in the pancreas of obese humans [8, 9, 11], rodents [12–16], and injury animal models [10]. Replication is the major mechanism for expanding the β-cell mass in adult mice [3, 4, 7].

When β-cell mass is decreased by a disruption of balance between cell growth (replication and neogenesis) and cell death, glucose intolerance develops. Indeed, human studies have shown reduced β cells with increased α-cell proportions in the islets and remarkable heterogeneity of morphological changes of islets in patients with type 2 diabetes mellitus and suggest that insufficient β-cell mass could be the basis of the impaired insulin secretion [9, 17–19]. Since the expansion of β-cell mass in vivo is crucial in the regeneration-based therapy of diabetes, it is important to investigate the physiological conditions and mechanisms that promote β-cell increase and survival.

Previous studies have shown the slight improvement of insulin release and the only partial increase of β-cell ratio in the islet in weakly β-cell damaged rats using low doses of streptozotocin (STZ), when treated with short-term injection of lente insulin [20, 21] and islet transplantation [22]. However, little is known about whether new β-cell formation occurs when β cells face being severely destroyed and hyperglycemia was restored by the long-acting insulin injection or islet transplantation. In addition, it is not clear whether replication of the remaining β cells or neogenesis contributes to the recovery of β-cell formation.

We therefore investigated the ability of β cells to have new formation when hyperglycemia was prolonged in which residual β cells were severely destroyed by high doses of STZ (180 mg/kg) and when normoglycemia was achieved thereafter.

Materials and methods

Animals and animal groups

Male C57BL/6 mice aged 8 weeks (24.8 ± 0.5 g) ($n = 27$) had a single i.p. injection of STZ (180 mg/kg; Sigma), freshly dissolved in sterile citrate buffer (pH 4.5) or sterile citrate buffer (pH 4.5) alone, according to the Animal Models of Diabetic Complications Consortium (AMDCC) protocol. Blood glucose levels were measured by an enzyme-electrode method with ONE TOUCH UltraVue (Johnson & Johnson K.K.) on whole blood taken from the tail vein. Only those mice with a blood glucose concentration greater than 400 mg/dl within 3 days were used as diabetics in the experiments. One week after STZ injection, the diabetic mice were then divided into three groups (STZ 1 week group, hyperglycemic STZ 8 weeks group, and transplanted group). STZ 1 week mice ($n = 4$) were killed 1 week after STZ injection to confirm the destruction of β cells. STZ 8 weeks mice ($n = 17$) sustained hyperglycemia and were killed after 8 weeks. Mice in the transplanted group ($n = 6$) received islet transplantation under the left kidney capsule, which sustained normoglycemia throughout the 8-week course of the experiment. Weight-matched 8-week-old male C57BL/6 mice were used as donors and recipients of islet grafts. For insulin injection study, animals ($n = 10$) were made diabetic by a single i.p. injection of the same dose of STZ (180 mg/kg). On days 3 and 7 after STZ injection, fed plasma glucose levels were measured, and the diabetic mice (22.1 ± 1.2 g) received twice-daily injections of the long-acting human analog, Detemir (NN304) [LysB29 (N^{ε}-tetradecanoyl) des (B30) insulin human] (1/10–1/50 U; Novo Nordisk) for 10 weeks. Detemir is designed to have a prolonged duration of action and provide a constant basal insulin supply due to its unique primary structure and mechanisms of reversible binding to plasma albumin and injection site [23–26]. The type and concentration of insulin were selected based on trial series such that the blood glucose level was in the normal range about 8–12 h/injection. Animals that kept normal blood glucose levels during the study were analyzed (Detemir injected group). Mice were housed in microisolator cages in a temperature-controlled room at 24 ± 2°C and at 50 ± 10% relative humidity under 12-h light/dark cycle. Standard rodent diet (CE-2; CLEA Japan, Inc., Tokyo, Japan) and water were supplied ad libitum. All animal experiments were approved by the Animal Care and Use Committee of Kyushu University, and mice were handled in accordance with guidelines for Animal experiments of Kyushu University.

Islet isolation and islet transplantation

Islet isolation and transplantation was performed as previously described in detail [27]. Islets were isolated by collagenase digestion, followed by separation on Ficoll gradients. After washing, 500 islets were handpicked and transplanted under the kidney capsule immediately. Implantation of islets was performed 1 week after STZ injection to STZ diabetic mice.

Histological study

Pancreases, kidney, and livers were fixed in 10% buffered formalin, embedded in paraffin, and cut in serial sections (2 μm). Kidney sections were stained with periodic acid-Schiff (PAS) and periodic acid-methenamine silver (PASM). Liver and pancreas sections were stained with hematoxylin and eosin (H&E) using standard histological procedures.

Immunohistochemistry

The following primary antibodies were used: anti-glucagon (1:500; Linco Research Inc.) and anti-insulin (1:500; DAKO), and Ki67 (1:1000; BD Pharmingen). Primary antibody was incubated overnight at 4°C and detected by immunofluorescence labeling with Alexa 488 or Alexa 568-conjugated secondary antibodies (1:200; Molecular Probes) or by immunoperoxidase with biotin-labeled secondary antibody (1:800; Vector Laboratories). Staining was visualized with diaminobenzidine. The sections were counterstained with hematoxylin. For proliferation studies, pancreatic sections (3–7 sections/animal) were double immunostained for insulin and Ki67. Images of all insulin-positive cells were captured on a Zeiss LSM 510 META confocal microscope in the confocal mode and were evaluated for expression of the cell cycle marker Ki67.

Measurements of serum variables

Blood was obtained from the heart immediately before isolation of the organs under pentobarbital anesthesia. Serum parameters were determined using the following methods: creatinine (high performance liquid chromatography; HPLC), albumin (BCG method), BUN (urease UV method), aspartate aminotransferase (AST), and alanine aminotransferase (ALT) (JSCC). Serum insulin was determined by enzyme-linked immunosorbent assay kit (Morinaga Institute of Biological Science, Yokohama, Japan). Total serum cholesterol (enzymatic assays) was determined by enzymatic assays (Wako Pure Chemical Industries Ltd., Japan).

Quantification of β cells and α cells

All islets, glucagon-positive, and insulin-positive cells on one full footprint section were photographed on the Keyence Biorevo microscope; 4–7 sections/animal at least 150 μm apart were evaluated. Each section was evaluated in pairs to match the quantification. Unpaired two-tailed Student's test was used for statistics. Data are presented as mean ± standard error of the mean (SEM). A P value of less than 0.05 was considered significant.

Results

STZ diabetic animals and treatment 1 (Detemir injection)

We examined the β-cell ability to increase when normoglycemia was achieved by injections of long-acting human insulin analog (Detemir). Animals were made diabetic by a single i.p. injection of the same dose of STZ (180 mg/kg body weight). It is known that STZ causes the preferential death of pancreatic β cells by its uptake in these cells via the GLUT-2 glucose transporter [28–30]. On days 3 and 7 after STZ injection, fed plasma glucose levels were measured to confirm hyperglycemia (>400 mg/dl within 3 days). After 1 week, the diabetic mice started receiving Detemir injections. Blood glucose levels were kept in normal range with twice-daily Detemir for 10 weeks (Fig. 1a). Blood glucose levels vary enormously along with Detemir injection, but twice-daily Detemir provided stable glycemic control during daytime (Fig. 1b). Seven days after STZ injection, animals showed slight loss of body weight, but at the time they were killed their body weight was not significantly different from that of the control mice (Fig. 2f).

To assess the changes in islet morphology, pancreatic sections were immunostained for insulin and glucagon. As shown in the multiple pictures (Fig. 1c), islets were severely disorganized; there were few β cells (green) and an increased proportion of α cells (red). This pattern did not differ with animals, indicating that β-cell mass and islet morphology were not recovered by Detemir injection.

STZ diabetic animals and treatment 2 (islet transplantation)

We then examined the β-cell ability to increase when normoglycemia was achieved by islet transplantation. Animals were made diabetic by a single i.p. injection of a high dose of STZ (180 mg/kg body weight). In this experiment, only those mice with hyperglycemia (>400 mg/dL) within 3 days were used. 1 week after STZ injection, these diabetic animals were divided into three groups, the hyperglycemic STZ 1 week group, hyperglycemic STZ 8 weeks group, and transplant group (Fig. 2a). The control group receiving citrate buffer alone was used as a positive control. For the transplant group, freshly isolated 500 islets were transplanted under kidney capsules (Fig. 2b).

Initially we investigated the effect of STZ on mice. Severe β-cell destruction (almost total absence of β cells) was determined by immunostaining for insulin and glucagon in STZ 1 week mice (Fig. 2c). There are few β cells (green) left with an increased proportion of α cells (red) in islets. Blood glucose levels were elevated after STZ injection and remained high during the study in STZ 8 weeks mice (Fig. 2d). The plasma insulin levels were considerably decreased, and body weight was markedly reduced in STZ 8 weeks mice (Fig. 2e, f). In STZ 8 weeks mice, similarly to STZ 1 week mice, there are few insulin-positive cells (green) left in islets, and reduced β cells remained throughout the 8-week course of the experiment

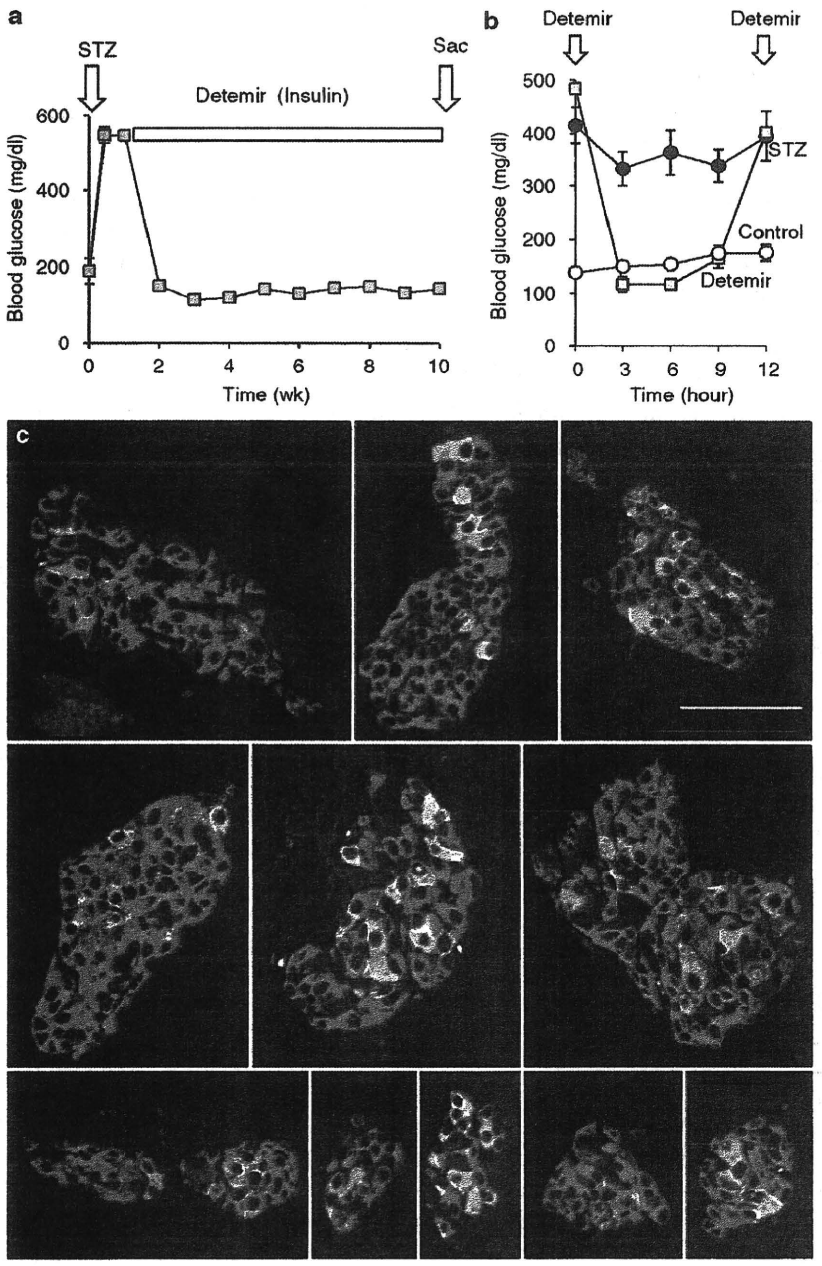

Fig. 1 Effect of Detemir injection. **a** Blood glucose levels in Detemir-injected mice. Animals were made diabetic by high doses of STZ (180 mg/kg body weight). On days 3 and 7 after STZ injection, fed plasma glucose levels were measured. Blood glucose levels of diabetic animals were kept in normal range with twice-daily injection for 10 weeks ($n = 6$). Glycemic control was stable, which is comparable to islet transplantation. **b** Glycemic excursion during daytime. Blood glucose levels of Detemir-injected mice ($n = 6$), STZ-treated mice ($n = 10$) and WT mice ($n = 10$) (from 9:30 a.m. to 9:30 p.m.). **c** No β-cell increase by Detemir treatment. Dual staining of insulin (*green*) and glucagon (*red*) was analyzed by confocal microscopy. All islets, small or large, were severely disorganized; this pattern did not differ with animals. *Scale bar* 50 μm

(Fig. 2g). The islets appeared severely disorganized with an increased proportion of glucagon-positive cells (Figs. 2g, 3), showing no β-cell increase in sustained hyperglycemia. Thus, the STZ mice displayed typical features of insulin deficiency, including loss of β cells and body weight, and low insulin content. In contrast, in transplanted mice, blood glucose levels were completely normalized and exhibited similar glycemic excursion to that of controls (Fig. 2d). The plasma insulin levels and body weight were increased after transplantation (Fig. 2e, f).

Furthermore, islet structure was greatly recovered (Figs. 2g, 3). The typical islet morphology of the core of insulin-positive cells with a mantle of glucagon-positive cells as seen in controls was found; this pattern did not differ with animals. Scattered singlets-doublets of insulin-positive cells were frequently observed in transplanted mice.

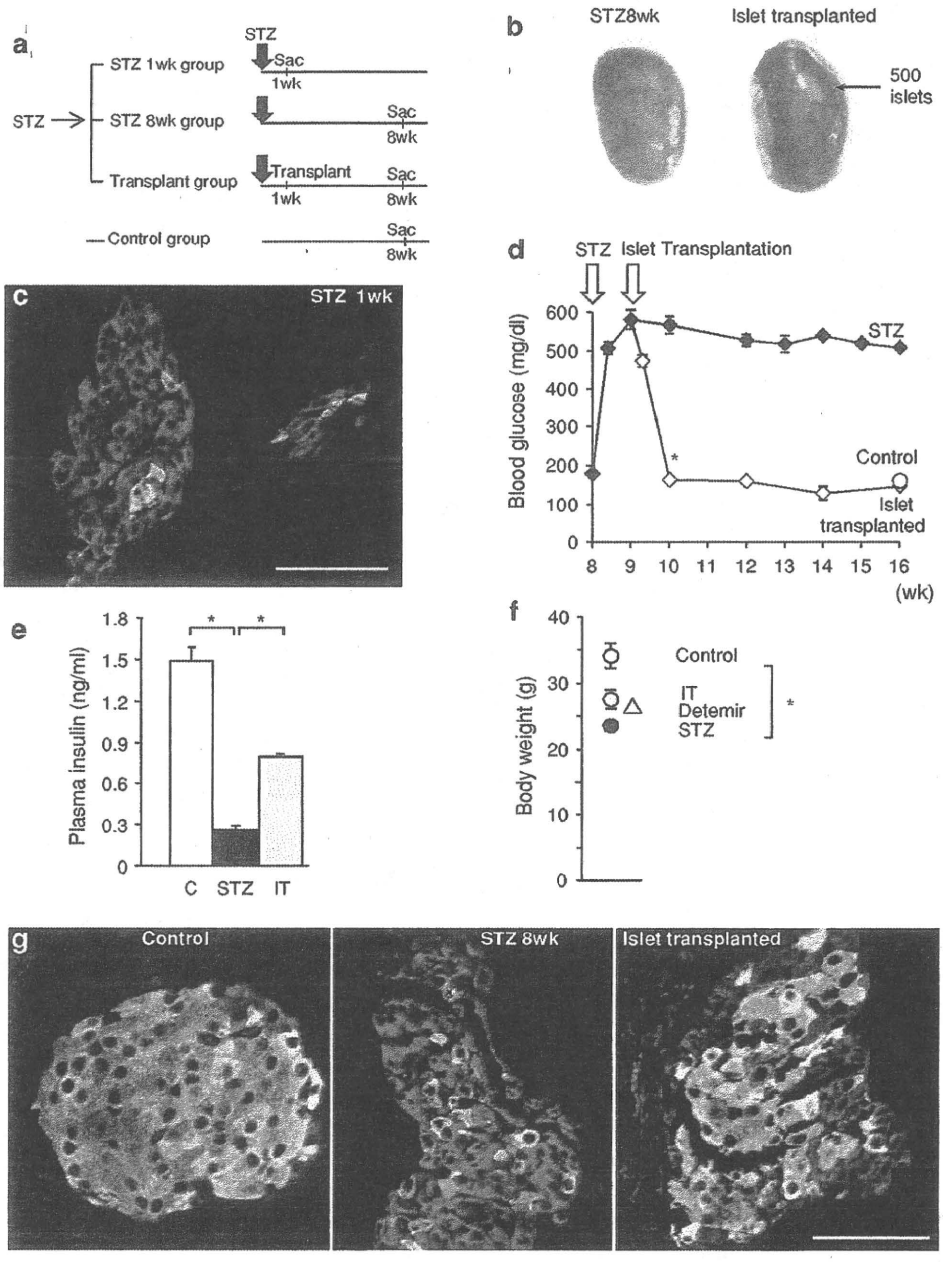

Fig. 2 Animal groups and effect of islet transplantation. **a** One week after STZ injection, animals made diabetic by a high dose of STZ (180 mg/kg body weight) were divided into three groups, STZ 1 week group ($n = 4$), STZ 8 weeks group ($n = 17$), and transplant group ($n = 6$). Control animals ($n = 4$). **b** A photograph of kidneys from mice with or without islet transplantation 8 weeks after a single i.p. STZ injection (180 mg/kg body weight). Freshly isolated 500 islets were transplanted under the kidney capsule (*arrow*). **c** Severely disorganized islets by STZ. Dual staining of pancreatic sections at 1 week after STZ injection with anti-insulin and anti-glucagon antibody was analyzed by confocal microscopy. There are few insulin-positive cells (*green*) left with an increased proportion of glucagon-positive cells (*red*). *Scale bar* 50 μm. Fed blood glucose levels (**d**), plasma insulin (**e**), body weight (**f**) of mice with or without transplantation at 16 weeks of age. **d** $*P < 0.05$ versus STZ 8 weeks mice. **g** No β-cell increase in sustained hyperglycemia in STZ 8 weeks mice and β-cell increase by islet transplantation. Dual staining of insulin (*green*) and glucagon (*red*) was analyzed by confocal microscopy. *Scale bar* 50 μm. Results are expressed as mean ± SEM. STZ-diabetic group (*black*), islet transplanted (IT) group (*gray*), control group (*white*). $*P < 0.05$

β-cell increase in the transplanted animals

To evaluate the β-cell increase, all insulin-positive cells on the cross section were photographed and counted. Compared to STZ 8 weeks mice, total β cells in the cross-section were increased in transplanted mice (Fig. 4a). Dividing by islet size, only small islets (6–20 β cells in the islet) were observed in the STZ mice group, while in islet transplanted mice, not only small islets but also many larger islets (21–100 and over 100 β cells) were found (Fig. 4b). To determine the changes of proportion of islets, all islets (collection of insulin-positive cells at least 6 cells in cross section) on the cross section were photographed, and the number of α cells and β cells in the islet were analyzed (Fig. 4c). In STZ 8 weeks mice, the ratio of β cells in the islet was reduced, and most of cells in the islet were α cells. These morphological abnormalities were not changed in hyperglycemia. In contrast, in transplanted mice, the ratio of β cells was recovered, as seen in control mice (Fig. 4c), indicating